SIAM J. APPL. MATH.
Vol. 70, No. 7, pp. 2627–2651

ON THE HYDRODYNAMIC DIFFUSION OF RIGID PARTICLES OF ARBITRARY SHAPE WITH APPLICATION TO DNA*

O. GONZALEZ† AND J. LI‡

Abstract. A general model for the diffusive dynamics of rigid particles in a viscous solvent is studied. The model applies to particles of arbitrary shape and allows for arbitrary cross- and self-coupling between translational and rotational degrees of freedom. Scaling and perturbation techniques are used to characterize the dynamics at time scales relevant to different classic experimental methods. It is shown that translational and rotational motion can be treated as independent at these time scales and can be described by simplified diffusion models, provided that certain geometric and hydrodynamic parameters associated with a particle are small. These parameters are estimated for DNA molecules of different length using a sequence-dependent geometric model based on x-ray crystallography and a numerical boundary element technique. Our results suggest that, for short DNA fragments up to about a persistence length, translational data can be accurately analyzed using a simplified model characterized by a scalar, orientationally averaged diffusion coefficient, but not rotational data. Indeed, the accurate analysis of rotational data may require a model which accounts for self-coupling and other possible effects at the rotational time scale.

Key words. hydrodynamic modeling, diffusion coefficients, diffusion tensors, orientational averaging, Stokes law, Stokes–Einstein relation

AMS subject classifications. 35Q70, 70E99, 76R50, 82C70, 92C05

DOI. 10.1137/090764219

1. Introduction.

Various experimental methods for probing the structure of rigid molecules in dilute solution are based on translational or rotational motion at diffusive time scales, for example, velocity sedimentation [14, 32, 35], dynamic light scattering [3, 34], electric dichroism and birefringence [13], and fluorescence polarization [40]. The interpretation of experimental data obtained from these methods relies on various simplifying assumptions about the dynamics of the molecules. The most basic of these is that translational and rotational motion can be treated as independent. In the translational case, it is traditionally assumed that the motion of a distinguished point in a molecule is described by an isotropic diffusion equation in a given spatial domain and characterized by a scalar diffusion coefficient corresponding to the average of those associated with translation along three principal axes [7, 37]. Similarly, in the rotational case, it is traditionally assumed that the motion of a distinguished axis in a molecule is described by an isotropic diffusion equation on the unit sphere and characterized by a scalar diffusion coefficient corresponding to rotation transverse to the axis [7, 13, 37].

The interpretation of experimental data also requires a geometric model for the hydrated surface of a molecule. Consistent with the dynamical assumptions, this surface has traditionally been modeled by a simple, symmetric shape such as an ellipsoid or a cylinder [7, 37]. For these shapes, translational and rotational motion are

*Received by the editors July 8, 2009; accepted for publication (in revised form) May 3, 2010; published electronically July 20, 2010. This research was supported by the National Science Foundation.

http://www.siam.org/journals/siap/70-7/76421.html

†Department of Mathematics, The University of Texas at Austin, Austin, TX 78712 (og@math.utexas.edu).

‡Graduate Program in Computational and Applied Mathematics, The University of Texas at Austin, Austin, TX 78712 (junli@ices.utexas.edu).

independent, and the traditional isotropic diffusion models can be expected to provide accurate descriptions of the independent motions in various cases. Indeed, we expect an isotropic model to accurately describe the translational motion of the center of a nearly spherical ellipsoid, as well as the rotational motion of the axis of a relatively elongated cylinder. Recently, however, hydrodynamic experiments have been used to estimate structural features of proteins [2, 6, 16] and DNA [1, 19, 26] using more realistic geometric models. Unlike ellipsoids and cylinders, these models are irregularly shaped and have no apparent symmetry. For such models, translational and rotational motion are generally coupled, and the traditional diffusion models which treat these motions as independent may no longer be accurate. Indeed, whereas the diffusional characteristics of a simple, symmetric shape are described by independent diffusion coefficients associated with translation and rotation along three principal axes, the characteristics of an irregular shape are described by a six-dimensional diffusion tensor with various different couplings [20, 21, 24].

In this article, we study the diffusive dynamics of rigid particles of arbitrary shape and examine the effect of various couplings at time scales relevant to different classic experimental methods. We consider the general model of hydrodynamic diffusion introduced by Brenner [4, 5], with arbitrary cross- and self-coupling between translational and rotational degrees of freedom, and we use techniques of perturbation theory to characterize the dynamics at different time scales. At scales relevant to experimental methods based on translation, we show, for a particle of arbitrary shape, that all cross- and self-coupling effects vanish in a leading-order approximation, provided only that a geometric parameter ϵ, defined as the dimensionless ratio of the characteristic size of the particle to that of the observed experimental domain, is small. In this case, the translational motion of any reference point in the particle is described by an isotropic diffusion equation. The equation is characterized by a scalar diffusion coefficient corresponding to the orientational average of the three-dimensional diffusion tensor associated with pure translation. Indeed, this coefficient characterizes the translational diffusion of not only symmetric and nearly spherical shapes, but also asymmetric and highly aspherical shapes as well. Thus the traditional isotropic model, with an appropriately defined translational diffusion coefficient, is expected to provide an accurate description of translational motion at the relevant time scales under an appropriate restriction on the size of a particle, with no restriction on its shape.

Different conclusions may be drawn for methods based on rotation. At time scales relevant to these methods, we show, for a particle of arbitrary shape, that all cross-coupling effects vanish in a leading-order approximation, provided as before that the geometric parameter ϵ is small. In this case, the rotational motion of the particle is described by a self-coupled diffusion equation on the space of three-dimensional rotations. Moreover, we show that certain self-coupling effects vanish, and the motion of any distinguished axis or unit vector n in the particle is described by an isotropic diffusion equation on the unit sphere, when additionally a shape-dependent hydrodynamic parameter ζ_n, defined as the dimensionless ratio of diffusion coefficients for rotation transverse and parallel to n, is small. The resulting equation on the unit sphere is characterized by a scalar diffusion coefficient corresponding to the orientational average, in the two-dimensional subspace orthogonal to the distinguished axis, of the three-dimensional diffusion tensor associated with pure rotation. Thus the traditional isotropic model on the unit sphere, with an appropriately defined transverse rotational diffusion coefficient, is expected to provide an accurate description of the rotational motion of a distinguished axis at the relevant time scales under appropriate restrictions on both the size and shape of a particle.

Various aspects of these results have been considered before. Brenner [4] studied cross-coupling between translational and rotational diffusion for a restricted class of shapes with no self-coupling. However, time scale and general coupling effects for arbitrary shapes were not considered. Berne and Pecora [3] studied self-coupling effects in the rotational diffusion of arbitrary shapes. However, time scale and cross-coupling effects between translational and rotational diffusion were not considered. The subject of rotational diffusion for different shapes in the absence of cross-coupling effects has been studied extensively, beginning with the pioneering work of Debye [8] and Perrin [30, 31], and continued in the works by Favro [12], McConnell [27], and the references therein. In this work, we use scaling and perturbation techniques to study arbitrary cross- and self-coupling effects for particles of arbitrary shape. We show that translational and rotational diffusion can be treated as independent at appropriate time scales, and can be described by traditional simplified models with appropriately defined coefficients, provided that the parameters ϵ and ζ_n introduced herein are small. Moreover, we study the properties of the diffusion coefficients that arise in the simplified models. Analogous to the center of diffusion which minimizes the translational diffusion coefficient [6, 21], we establish the existence of an axis of diffusion which minimizes the transverse rotational diffusion coefficient.

As an application of our results, we examine various classic hydrodynamic methods for probing the structure of short DNA molecules up to about a persistence length, which corresponds to about 150 basepairs [33]. We restrict our attention to this length scale since the rigidity assumption in the present theory becomes more of an issue at longer lengths. We estimate the parameters ϵ and ζ_n for DNA in this length range using a sequence-dependent geometric model based on x-ray crystallography and a numerical boundary element technique described in detail elsewhere [18, 19]. Our results show that, for translational methods such as velocity sedimentation and dynamic light scattering, the parameter ϵ is small for any sequence, which suggests that the translational motion measured by these methods is accurately described by the traditional isotropic model. In contrast, for rotational methods such as electric dichroism and birefringence, as well as fluorescence polarization, the parameter ζ_n is highly variable and can be close to order unity depending on the sequence, which suggests that the rotational motion measured by these methods may not be accurately described by the traditional isotropic model. Thus, for short DNA molecules up to about a persistence length, the use of a more realistic geometric model is compatible with traditional assumptions made in the analysis of translational data, but not rotational data. Indeed, the accurate analysis of rotational data may require a diffusion model which accounts for self-coupling and other possible effects at the rotational time scale.

The presentation is organized as follows. In section 2, we outline a general, fully coupled model of hydrodynamic diffusion of rigid particles and establish notation. In section 3, we outline an initial-boundary value problem for the general diffusion model, derive our main results on translational and rotational diffusion at different time scales, and study various properties of the scalar coefficients arising in the simplified models. In section 4, we use our results to examine various classic hydrodynamic methods for studying DNA.

2. Theory. Here we outline a model introduced by Brenner [4, 5] for the diffusion of rigid particles of arbitrary shape in a viscous solvent. The final form of the model is a convection-diffusion equation on a six-dimensional space of particle positions and orientations; see (2.40) below. We give a careful summary of the hydromechanical basis of the model, highlight and clarify various inherent approximations, and establish

notation and results that are necessary for its physical and mathematical interpretation.

2.1. Hydromechanical relations. Consider a single, rigid particle of arbitrary shape immersed in a viscous solvent and moving under the action of various external forces. The configuration of the particle is specified by the location of a reference point $\boldsymbol{r}$ fixed in the particle, and the orientation of a right-handed, orthonormal frame $\{\boldsymbol{d}_i\}$ $(i = 1, 2, 3)$ attached to the particle. The kinematics of the particle relative to a right-handed, orthonormal experimental reference frame $\{\boldsymbol{e}_i\}$ are encapsulated in the relations

$$\dot{\boldsymbol{r}} = \boldsymbol{v}, \quad \dot{\boldsymbol{d}}_i = \boldsymbol{\omega} \times \boldsymbol{d}_i, \tag{2.1}$$

where $\boldsymbol{v}$ is the velocity of the particle reference point, $\boldsymbol{\omega}$ is the angular velocity of the particle frame, an overdot denotes a derivative with respect to time holding $\{\boldsymbol{e}_i\}$ fixed, and $\times$ denotes the standard cross product.

We assume that the particle is relatively large compared to the solvent molecules and that its velocities $(\boldsymbol{v}, \boldsymbol{\omega})$ can be decomposed into a sum of rapidly fluctuating velocities $(\boldsymbol{v}', \boldsymbol{\omega}')$ due to thermal effects, and slowly varying velocities $(\overline{\boldsymbol{v}}, \overline{\boldsymbol{\omega}})$ due to external effects, namely,

$$\boldsymbol{v} = \boldsymbol{v}' + \overline{\boldsymbol{v}}, \quad \boldsymbol{\omega} = \boldsymbol{\omega}' + \overline{\boldsymbol{\omega}}. \tag{2.2}$$

We assume that the velocities $(\boldsymbol{v}', \boldsymbol{\omega}')$ have vanishing means in the sense that their time averages, taken over any window that is sufficiently large compared to the characteristic molecular collision time, are negligibly small. In this case, the velocities $(\overline{\boldsymbol{v}}, \overline{\boldsymbol{\omega}})$ can be identified as the time averages of $(\boldsymbol{v}, \boldsymbol{\omega})$ over a local, moving window in time. We assume that $(\overline{\boldsymbol{v}}, \overline{\boldsymbol{\omega}})$ and the window size are sufficiently small so that the body configuration can be approximated as constant in the window. As a consequence, $(\overline{\boldsymbol{v}}, \overline{\boldsymbol{\omega}})$ are objective in the sense that their components in the particle and experimental frames are related through the usual transformation laws for a change of frame.

We denote the net external force and torque on the particle by $(\boldsymbol{f}^{\text{ext}}, \boldsymbol{\tau}^{\text{ext}})$, where the torque is referred to the particle reference point. We assume that $(\boldsymbol{f}^{\text{ext}}, \boldsymbol{\tau}^{\text{ext}})$ depend on the configuration of the particle, but not its linear or angular velocities. Moreover, we assume that

$$\boldsymbol{f}^{\text{ext}} = \boldsymbol{f}^0 + \boldsymbol{f}^\rho, \quad \boldsymbol{\tau}^{\text{ext}} = \boldsymbol{\tau}^0 + \boldsymbol{\tau}^\rho, \tag{2.3}$$

where $(\boldsymbol{f}^0, \boldsymbol{\tau}^0)$ are net loads associated with body (distributed) and point (concentrated) forces of any type except osmotic, and $(\boldsymbol{f}^\rho, \boldsymbol{\tau}^\rho)$ are net loads associated with forces of osmotic type, which will be described later. Assuming that the particle and solvent have uniform mass densities, and that all body force fields are conservative, we have

$$\boldsymbol{f}^0 = m_b \boldsymbol{f}^{\text{body}} + \boldsymbol{f}^{\text{point}}, \quad \boldsymbol{\tau}^0 = m_b \boldsymbol{\tau}^{\text{body}} + \boldsymbol{\tau}^{\text{point}}, \tag{2.4}$$

where m_b is the buoyant mass of the particle in the solvent, $(\boldsymbol{f}^{\text{body}}, \boldsymbol{\tau}^{\text{body}})$ are net body loads per unit mass, and $(\boldsymbol{f}^{\text{point}}, \boldsymbol{\tau}^{\text{point}})$ are net point loads.

We assume that the time-averaged velocities of a particle are entirely determined by the net external loads acting on it. Specifically, we assume a general linear relation of the form

$$\overline{\boldsymbol{v}} = \boldsymbol{M}_1 \boldsymbol{f}^{\text{ext}} + \boldsymbol{M}_3 \boldsymbol{\tau}^{\text{ext}}, \quad \overline{\boldsymbol{\omega}} = \boldsymbol{M}_2 \boldsymbol{f}^{\text{ext}} + \boldsymbol{M}_4 \boldsymbol{\tau}^{\text{ext}}, \tag{2.5}$$

where $\boldsymbol{M}_1, \ldots, \boldsymbol{M}_4$ are given hydrodynamic mobility tensors. Consistent with the assumptions on the smallness and slowly varying nature of the velocities $(\overline{\boldsymbol{v}}, \overline{\boldsymbol{\omega}})$, these relations are assumed to be objective in the sense that they hold without modification in both the particle and experimental frames. That is, any induced forces caused by the relative translation and rotation of these frames are assumed to be negligible when averaged in time. These relations are consistent with a Stokesian hydrodynamic model of the solvent and are a generalization, to a rigid particle of arbitrary shape, of the classic Stokes laws for the force and torque on a sphere. In general, the mobility tensors may depend on the configuration of the particle as well as the choice of reference point and frame fixed in the particle [15, 19, 20, 21, 24].

Various considerations arise in applications in which the experimental frame is rotating. In this case, the particle velocities must be interpreted as relative velocities, and the net body loads must be augmented to account for acceleration effects induced by rotation. Assuming that the experimental frame $\{\boldsymbol{e}_i\}$ rotates with a slowly varying angular velocity $\boldsymbol{\zeta}$, and that the particle velocities $(\overline{\boldsymbol{v}}, \overline{\boldsymbol{\omega}})$ are small, we neglect angular acceleration and Coriolis effects and consider only centrifugal effects. Accordingly, we augment $\boldsymbol{f}^{\text{body}}$ with the term $-\boldsymbol{\zeta} \times (\boldsymbol{\zeta} \times \boldsymbol{r})$, and augment $\boldsymbol{\tau}^{\text{body}}$ with the term $-\boldsymbol{\zeta} \times (\boldsymbol{\Gamma}\boldsymbol{\zeta})$, where $\boldsymbol{\Gamma}$ is the rotational inertia tensor [17, 23] of the particle per unit mass about the reference point $\boldsymbol{r}$.

2.2. Component form. The hydromechanical relations outlined above involve vector and tensor quantities which are defined independently of any frame. We next express these quantities in terms of a convenient set of components in the experimental frame $\{\boldsymbol{e}_i\}$ and the particle frame $\{\boldsymbol{d}_i\}$. To begin, let $r \in \mathbb{R}^3$ and $Q \in \mathbb{R}^{3\times 3}$ denote the components of $\boldsymbol{r}$ and $\{\boldsymbol{d}_i\}$ in the frame $\{\boldsymbol{e}_i\}$, where $r_i = \boldsymbol{e}_i \cdot \boldsymbol{r}$, $Q_{ij} = \boldsymbol{e}_i \cdot \boldsymbol{d}_j$, and a dot denotes the standard dot product. In terms of these components, we have

$$\boldsymbol{r} = r_i \boldsymbol{e}_i, \quad \boldsymbol{d}_j = Q_{ij} \boldsymbol{e}_i. \tag{2.6}$$

Here and throughout we use the usual summation convention on pairs of repeated indices. Notice that because $\{\boldsymbol{d}_i\}$ and $\{\boldsymbol{e}_i\}$ are right-handed, orthonormal frames, we have $Q \in \mathrm{SO}_3$, where $\mathrm{SO}_3 \subset \mathbb{R}^{3\times 3}$ is the set of proper, three-dimensional rotation matrices, namely, $Q^T = Q^{-1}$ and $\det Q = 1$. Thus the configuration of a particle is uniquely defined by an element $(r, Q) \in \mathbb{R}^3 \times \mathrm{SO}_3$.

Let $V, V', \overline{V} \in \mathbb{R}^3$ and $\Omega, \Omega', \overline{\Omega} \in \mathbb{R}^3$ denote linear and angular velocity components in the frame $\{\boldsymbol{d}_i\}$, defined by $V_i = \boldsymbol{v} \cdot \boldsymbol{d}_i$, $V_i' = \boldsymbol{v}' \cdot \boldsymbol{d}_i$, $\overline{V_i} = \overline{\boldsymbol{v}} \cdot \boldsymbol{d}_i$, and so on. Then the kinematical equations in (2.1) and (2.2) take the form

$$\begin{aligned} \dot{r} &= QV, \quad \dot{Q} = Q[\Omega\times], \\ V &= V' + \overline{V}, \quad \Omega = \Omega' + \overline{\Omega}, \end{aligned} \tag{2.7}$$

where for any vector $\Omega \in \mathbb{R}^3$ we define a skew-symmetric matrix $[\Omega\times] \in \mathbb{R}^{3\times 3}$ by

$$[\Omega\times] = \begin{pmatrix} 0 & -\Omega_3 & \Omega_2 \\ \Omega_3 & 0 & -\Omega_1 \\ -\Omega_2 & \Omega_1 & 0 \end{pmatrix}. \tag{2.8}$$

By definition, this matrix satisfies $[\Omega\times]g = \Omega \times g$ for all $g \in \mathbb{R}^3$. For any skew-symmetric matrix $W \in \mathbb{R}^{3\times 3}$ it will be convenient to define a vector $\mathrm{vec}[W] \in \mathbb{R}^3$ by

$$\mathrm{vec}[W] = \begin{pmatrix} W_{32} \\ W_{13} \\ W_{21} \end{pmatrix}. \tag{2.9}$$

By definition, this vector satisfies $\mathrm{vec}[W] \times g = Wg$ for all $g \in \mathbb{R}^3$, and by combining (2.8) and (2.9), we find $\mathrm{vec}[g\times] = g$. In indicial notation, we have $[\Omega\times]_{ij} = \epsilon_{ikj}\Omega_k$ and $\mathrm{vec}_j[W] = \frac{1}{2}\epsilon_{ijk}W_{ik}$, where ϵ_{ijk} is the permutation symbol of vector analysis. In later developments, we will make use of the standard epsilon-delta identity $\epsilon_{ijk}\epsilon_{mnk} = \delta_{im}\delta_{jn} - \delta_{in}\delta_{jm}$, where δ_{ij} is the Kronecker delta symbol.

Let $F^{\mathrm{ext}}, F^0, F^\rho \in \mathbb{R}^3$ and $T^{\mathrm{ext}}, T^0, T^\rho \in \mathbb{R}^3$ denote force and torque components in the frame $\{\boldsymbol{d}_i\}$, defined by $F_i^{\mathrm{ext}} = \boldsymbol{f}^{\mathrm{ext}} \cdot \boldsymbol{d}_i$, $F_i^0 = \boldsymbol{f}^0 \cdot \boldsymbol{d}_i$, $F_i^\rho = \boldsymbol{f}^\rho \cdot \boldsymbol{d}_i$, and so on. Then the load relations in (2.3) take the form

$$F^{\mathrm{ext}} = F^0 + F^\rho, \quad T^{\mathrm{ext}} = T^0 + T^\rho. \tag{2.10}$$

We note that the body and point load relations in (2.4) take a similar form in similar components. Throughout our developments, we will also consider the force and torque components $f^{\mathrm{ext}}, f^0, f^\rho \in \mathbb{R}^3$ and $\tau^{\mathrm{ext}}, \tau^0, \tau^\rho \in \mathbb{R}^3$ in the experimental frame $\{\boldsymbol{e}_i\}$, defined by $f_i^{\mathrm{ext}} = \boldsymbol{f}^{\mathrm{ext}} \cdot \boldsymbol{e}_i$, $f_i^0 = \boldsymbol{f}^0 \cdot \boldsymbol{e}_i$, $f_i^\rho = \boldsymbol{f}^\rho \cdot \boldsymbol{e}_i$, and so on. These components satisfy a relation analogous to (2.10). Moreover, in view of (2.6), they are related to the previous components through a standard change of frame relation. Specifically, omitting the superscripts for brevity, we have

$$\begin{pmatrix} F \\ T \end{pmatrix} = \mathbb{Q}^T \begin{pmatrix} f \\ \tau \end{pmatrix}, \tag{2.11}$$

where $\mathbb{Q} \in \mathbb{R}^{6\times 6}$ is a change of frame matrix defined as

$$\mathbb{Q} = \begin{pmatrix} Q & 0 \\ 0 & Q \end{pmatrix}. \tag{2.12}$$

Let $M_a \in \mathbb{R}^{3\times 3}$ $(a = 1, \ldots, 4)$ denote the components of the mobility tensors $\boldsymbol{M}_a$ in the frame $\{\boldsymbol{d}_i\}$, defined by $(M_a)_{ij} = \boldsymbol{d}_i \cdot \boldsymbol{M}_a \boldsymbol{d}_j$. Then the hydrodynamic relations in (2.5) take the form

$$\overline{V} = M_1 F^{\mathrm{ext}} + M_3 T^{\mathrm{ext}}, \quad \overline{\Omega} = M_2 F^{\mathrm{ext}} + M_4 T^{\mathrm{ext}}. \tag{2.13}$$

For convenience, we introduce an overall mobility matrix $M \in \mathbb{R}^{6\times 6}$ by

$$M = \begin{pmatrix} M_1 & M_3 \\ M_2 & M_4 \end{pmatrix}. \tag{2.14}$$

Assuming a standard Stokesian hydrodynamic model [15, 19, 20, 21, 24], the matrix M is constant, symmetric, and positive-definite. The first property is frame-dependent and holds only in the particle frame, which motivates our use of that frame, whereas the latter two properties are frame-independent. Thus the overall matrix satisfies $M^T = M > 0$, which implies that its block entries satisfy $M_1^T = M_1 > 0$, $M_4^T = M_4 > 0$, and $M_2 = M_3^T$.

For a standard Stokesian model, the matrix M also satisfies a simple transformation law under a change of particle reference point and particle frame. Indeed, let $(\boldsymbol{r}', \boldsymbol{d}_i')$ and $(\boldsymbol{r}, \boldsymbol{d}_i)$ be two arbitrary points and frames fixed in the particle, and let $\xi \in \mathbb{R}^3$ and $\Xi \in \mathrm{SO}_3$ be the components of the relative displacement and rotation defined such that $\boldsymbol{r}' = \boldsymbol{r} + \xi_i \boldsymbol{d}_i$ and $\boldsymbol{d}_j' = \Xi_{ij}\boldsymbol{d}_i$. Then the associated component matrices M' and M satisfy [21]

$$M' = \mathbb{T}^T M \mathbb{T}, \tag{2.15}$$

where $\mathbb{T} \in \mathbb{R}^{6\times 6}$ is a transformation matrix defined in partitioned form by

$$\mathbb{T} = \begin{pmatrix} \Xi & 0 \\ [\xi\times]\Xi & \Xi \end{pmatrix}. \tag{2.16}$$

Combining (2.14) and (2.15) we find that the blocks of M' and M satisfy

$$\begin{aligned} M_1' &= \Xi^T\Big(M_1 + M_3[\xi\times] + [\xi\times]^T M_2 + [\xi\times]^T M_4[\xi\times]\Big)\Xi, \\ M_2' &= (M_3')^T = \Xi^T\Big(M_2 + M_4[\xi\times]\Big)\Xi, \\ M_4' &= \Xi^T M_4 \Xi. \end{aligned} \tag{2.17}$$

2.3. Local coordinates. It will be convenient to formulate the hydromechanical relations of the previous section in local coordinates. To this end, we consider an arbitrary, local coordinate chart on the space of configurations $(r, Q) \in \mathbb{R}^3 \times \mathrm{SO}_3$ of the form

$$r = \psi(q), \quad Q = \phi(\eta), \tag{2.18}$$

where $(q, \eta) \in \mathbb{R}^3\times\mathbb{R}^3$. We assume that (ψ, ϕ) is a smooth bijection between some open subset of $\mathbb{R}^3\times\mathbb{R}^3 = \mathbb{R}^6$ and some open subset of $\mathbb{R}^3\times\mathrm{SO}_3$. Thus to each configuration (r, Q) in the image of the chart we associate a unique local representation (q, η).

For any time-dependent curve of configurations, the linear and angular velocity components $(V, \Omega) \in \mathbb{R}^6$ have a unique local representation $\mathcal{V} \in \mathbb{R}^6$. Indeed, from (2.7) and (2.18) we find

$$V = Q^T\dot{r} = Q^T\nabla_q\psi\dot{q}, \quad \Omega = \mathrm{vec}[Q^T\dot{Q}] = S\dot{\eta}, \tag{2.19}$$

where $\nabla_q\psi(q) \in \mathbb{R}^{3\times 3}$ is the Jacobian matrix of $\psi(q)$, and $S(\eta) \in \mathbb{R}^{3\times 3}$ is a structure matrix associated with $\phi(\eta)$ given by

$$S_{mj} = \mathrm{vec}_m\left[Q^T\frac{\partial Q}{\partial \eta_j}\right] = \frac{1}{2}\epsilon_{imk}\phi_{li}\frac{\partial \phi_{lk}}{\partial \eta_j}. \tag{2.20}$$

Consistent with the assumption that (ψ, ϕ) is a bijection, we assume that the matrices $\nabla_q\psi$ and S are invertible. Thus, for any given curve of configurations, the components (V, Ω) are uniquely determined by the coordinate derivatives $(\dot{q}, \dot{\eta})$, with the converse also being true. Writing (2.19) in matrix form, we get

$$\begin{pmatrix} V \\ \Omega \end{pmatrix} = \Lambda\mathcal{V}, \tag{2.21}$$

where $\Lambda(q, \eta) \in \mathbb{R}^{6\times 6}$ is a velocity connection matrix and $\mathcal{V} \in \mathbb{R}^6$ is a local velocity vector defined as

$$\Lambda = \begin{pmatrix} Q^T\nabla_q\psi & 0 \\ 0 & S \end{pmatrix}, \quad \mathcal{V} = \begin{pmatrix} \dot{q} \\ \dot{\eta} \end{pmatrix}. \tag{2.22}$$

Analogous to the decomposition of (V, Ω), we assume that the local representation $\mathcal{V}$ can be decomposed into the sum of a rapidly fluctuating part $\mathcal{V}'$ and a slowly varying part $\overline{\mathcal{V}}$ as

$$\mathcal{V} = \mathcal{V}' + \overline{\mathcal{V}}. \tag{2.23}$$

We assume that $\mathcal{V}'$ has a vanishing mean so that $\overline{\mathcal{V}}$ can be identified as the time average of $\mathcal{V}$ over a local, moving window in time. Taking the time average of (2.21), treating the configuration variables as constant in the averaging window, we find

$$\begin{pmatrix} \overline{V} \\ \overline{\Omega} \end{pmatrix} = \Lambda \overline{\mathcal{V}}. \tag{2.24}$$

Just as the velocity components, the external load components also have a unique local representation. To any arbitrary load components $(F, T) \in \mathbb{R}^6$ we associate a local representation $\mathcal{F} \in \mathbb{R}^6$ via the expression

$$\mathcal{F} \cdot \mathcal{V} = \begin{pmatrix} F \\ T \end{pmatrix} \cdot \begin{pmatrix} V \\ \Omega \end{pmatrix} \quad \forall \begin{pmatrix} V \\ \Omega \end{pmatrix} = \Lambda \mathcal{V}. \tag{2.25}$$

From this we deduce, by the arbitrariness of $\mathcal{V}$,

$$\mathcal{F} = \Lambda^T \begin{pmatrix} F \\ T \end{pmatrix} = \Lambda^T \mathbb{Q}^T \begin{pmatrix} f \\ \tau \end{pmatrix}. \tag{2.26}$$

The first equality follows directly from (2.25), whereas the second follows from (2.11). Thus the local representation $\mathcal{F}$ of an arbitrary load can be written in terms of components (F, T) in the particle frame, or components (f, τ) in the experimental frame.

The local form of the hydrodynamic relations can now be derived. Substituting (2.26) and (2.24) into (2.13) we obtain

$$\overline{\mathcal{V}} = \mathcal{M} \mathcal{F}^{\text{ext}}, \tag{2.27}$$

where $\mathcal{F}^{\text{ext}}$ is the local representation of the load $(F^{\text{ext}}, T^{\text{ext}})$ and $\mathcal{M} \in \mathbb{R}^{6\times 6}$ is a local representation of the hydrodynamic matrix M defined by

$$\mathcal{M} = \Lambda^{-1} M \Lambda^{-T}. \tag{2.28}$$

If we partition $\mathcal{M}$ into blocks $\mathcal{M}_a \in \mathbb{R}^{3\times 3}$ as in (2.14), then from (2.28) and (2.22) we find

$$\begin{pmatrix} \mathcal{M}_1 & \mathcal{M}_3 \\ \mathcal{M}_2 & \mathcal{M}_4 \end{pmatrix} = \begin{pmatrix} \nabla_q \psi^{-1} Q M_1 Q^T \nabla_q \psi^{-T} & \nabla_q \psi^{-1} Q M_3 S^{-T} \\ S^{-1} M_2 Q^T \nabla_q \psi^{-T} & S^{-1} M_4 S^{-T} \end{pmatrix}. \tag{2.29}$$

A related matrix that will arise in later discussions is $\mathcal{C} = \mathcal{M} \Lambda^T \mathbb{Q}^T \in \mathbb{R}^{6\times 6}$. For future reference, we note that the partitioned form of this matrix is

$$\begin{pmatrix} \mathcal{C}_1 & \mathcal{C}_3 \\ \mathcal{C}_2 & \mathcal{C}_4 \end{pmatrix} = \begin{pmatrix} \nabla_q \psi^{-1} Q M_1 Q^T & \nabla_q \psi^{-1} Q M_3 Q^T \\ S^{-1} M_2 Q^T & S^{-1} M_4 Q^T \end{pmatrix}. \tag{2.30}$$

2.4. Admissible configurations. Throughout our studies, we assume that the solvent in which one or more particles are immersed occupies a fixed, bounded domain $\mathrm{E} \subset \mathbb{R}^3$ in Cartesian coordinates in the experimental frame $\{\boldsymbol{e}_i\}$. Accordingly, we define the space of admissible configurations (r, Q) for each particle to be $\mathrm{E} \times \mathrm{SO}_3$. Inherent in this definition is the assumption that particles are always well separated and are small compared to the size of the domain. We will always assume this to be the case; a more sophisticated definition which accounts for the finite size of the particles and steric effects between them would be necessary otherwise.

We consider an arbitrary, local coordinate chart $\Phi : \mathcal{E} \times \mathcal{A} \to \mathrm{E} \times \mathrm{SO}_3$ of the form

$$(r, Q) = \Phi(q, \eta) = (\psi(q), \phi(\eta)), \tag{2.31}$$

where $\mathcal{E}$ and $\mathcal{A}$ are subsets of $\mathbb{R}^3$. We assume that $\mathcal{E}$ and $\mathcal{A}$ are open and bounded with piecewise smooth boundaries, and that Φ is a smooth bijection onto its image. Moreover, we assume that the image of Φ has full measure in $\mathrm{E}\times\mathrm{SO}_3$. This assumption is made purely for convenience and will allow us to state all results in terms of a single chart Φ rather than an atlas of overlapping charts which covers the entirety of $\mathrm{E}\times\mathrm{SO}_3$.

The set $\mathrm{E} \times \mathrm{SO}_3$ can be viewed as a six-dimensional manifold in the Euclidean space $\mathbb{R}^{12}$. Indeed, $\mathrm{E} \times \mathrm{SO}_3$ is the Cartesian product of the three-dimensional manifolds $\mathrm{E} \subset \mathbb{R}^3$ and $\mathrm{SO}_3 \subset \mathbb{R}^{3\times3} = \mathbb{R}^9$. In terms of the chart Φ, the intrinsic six-volume of a subset $B \subset \mathrm{E} \times \mathrm{SO}_3$ is given by [28, 38]

$$\mathrm{vol}(B) = \int_{\mathcal{B}} g \, dV, \quad g = \sqrt{\det[\nabla\Phi^T \nabla\Phi]}, \tag{2.32}$$

where $\mathcal{B} \subset \mathcal{E} \times \mathcal{A}$ is the preimage of B under Φ, $dV = dV_q dV_\eta$ is the standard volume element in $\mathcal{E} \times \mathcal{A}$, and $\nabla\Phi(q, \eta) \in \mathbb{R}^{12\times6}$ denotes the Jacobian matrix of $\Phi(q, \eta)$ viewed as a map from $\mathbb{R}^6$ into $\mathbb{R}^{12}$. From the structure of Φ given in (2.31) we find

$$g = g_q g_\eta, \quad g_q = \sqrt{\det[\nabla_q\psi^T \nabla_q\psi]}, \quad g_\eta = \sqrt{\det[\nabla_\eta\phi^T \nabla_\eta\phi]}, \tag{2.33}$$

where $\nabla_q\psi(q) \in \mathbb{R}^{3\times3}$ and $\nabla_\eta\phi(\eta) \in \mathbb{R}^{9\times3}$ denote the Jacobian matrices of $\psi(q)$ and $\phi(\eta)$, with the latter viewed as a map from $\mathbb{R}^3$ into $\mathbb{R}^9$.

From the assumption that Φ is a smooth bijection onto its image, it follows that $g > 0$ in $\mathcal{E} \times \mathcal{A}$. However, from the assumption that Φ has full measure, it follows that $g = 0$ at some points on $\partial(\mathcal{E} \times \mathcal{A}) = (\partial\mathcal{E} \times \mathcal{A}) \cup (\mathcal{E} \times \partial\mathcal{A})$. Indeed, by intrinsic properties of the set SO_3, we must necessarily have $g_\eta = 0$ on some portion of $\partial\mathcal{A}$. Moreover, it may also happen that $g_q = 0$ on some portion of $\partial\mathcal{E}$, as occurs, for example, when cylindrical or spherical coordinates are used to represent domains in Cartesian coordinates. Points at which $g = 0$ will be referred to as singular points of the chart Φ.

2.5. Diffusion model. We consider a dilute solution in which a solvent and a large number of identical but arbitrarily shaped solute particles occupy a domain E. To each solute particle $\mathcal{P}^a$ $(a = 1, \ldots, N)$ we associate a point $(q, \eta)^a \in \mathcal{E} \times \mathcal{A}$ which describes the position and orientation of the particle at time $t \geq 0$. We invoke the continuum approximation and assume that, at any instant, the points $(q, \eta)^a$ are continuously distributed with number density $\rho : \mathcal{E} \times \mathcal{A} \to \mathbb{R}$ with respect to the intrinsic volume element $g dV$. Thus the number or mass of particles with positions and orientations in a subset $\mathcal{B} \subset \mathcal{E} \times \mathcal{A}$ is given by

$$\mathrm{mass}(B) = \int_{\mathcal{B}} \rho g \, dV. \tag{2.34}$$

We employ the image set B on the left-hand side of (2.34) to emphasize the fact that ρ represents the density of particles per unit volume of the configuration space $\mathrm{E}\times\mathrm{SO}_3$. Indeed, when ρ is uniform, we see from (2.34) and (2.32) that the masses of any two subsets are equal when their intrinsic volumes are equal.

To each solute particle $\mathcal{P}^a$ we associate a vector $\overline{\mathcal{V}}^a \in \mathbb{R}^6$ which describes the time-averaged velocity of the particle at time $t \geq 0$. In the continuum approximation,

we assume that these velocities are modeled at any instant by a field $\overline{\mathcal{V}} : \mathcal{E} \times \mathcal{A} \to \mathbb{R}^6$, where $\overline{\mathcal{V}}(q, \eta)$ is the time-averaged velocity of the particle whose current coordinates are (q, η). In a similar manner, the amplitude or variance of the rapidly fluctuating, zero-mean velocity of each particle at any instant can be modeled by a temperature field $\Theta : \mathcal{E} \times \mathcal{A} \to \mathbb{R}$, which we assume to be uniform and constant. Moreover, we assume that the net external load on each particle at any instant can be modeled by a field $\mathcal{F}^{\text{ext}} : \mathcal{E} \times \mathcal{A} \to \mathbb{R}^6$. In view of (2.3) and (2.10), we have

$$\mathcal{F}^{\text{ext}} = \mathcal{F}^0 + \mathcal{F}^\rho, \tag{2.35}$$

where $\mathcal{F}^0$ is a net load associated with body and point forces of any type except osmotic, and $\mathcal{F}^\rho$ is a net load associated with forces of osmotic type due to gradients in the particle density. Specifically, in view of (2.26), we assume

$$\mathcal{F}^0 = \Lambda^T \mathbb{Q}^T \begin{pmatrix} f^0 \\ \tau^0 \end{pmatrix}, \quad \mathcal{F}^\rho = -\nabla \mu, \tag{2.36}$$

where (f^0, τ^0) are net load components in the experimental frame and $\mu = k\Theta \ln(\rho/\rho_*)$ is the chemical potential associated with ρ. Here k is the Boltzmann constant, ρ_* is a normalizing constant, and $\nabla = (\nabla_q, \nabla_\eta)$ is the standard gradient operator with respect to the coordinates (q, η) as employed earlier.

A basic equation describing the distribution of solute particles in a dilute solution can now be derived. Indeed, consider a distribution with density field ρ moving with an arbitrary velocity field $\overline{\mathcal{V}}$. Assuming that particles can be neither created nor destroyed, we deduce from (2.34) that the scaled density ρg must satisfy a standard conservation of mass equation in the Euclidean space $\mathcal{E} \times \mathcal{A}$, namely, $\partial(\rho g)/\partial t + \nabla \cdot (\rho g \overline{\mathcal{V}}) = 0$. Introducing the mass flux field $J = \rho \overline{\mathcal{V}} \in \mathbb{R}^6$, and dividing through by the Jacobian factor $g > 0$, which is independent of time, we obtain

$$\frac{\partial \rho}{\partial t} + g^{-1} \nabla \cdot (gJ) = 0. \tag{2.37}$$

Substituting (2.36) and (2.35) into the hydrodynamic relation (2.27), we find that the mass flux J takes the form

$$J = -\mathcal{D} \nabla \rho + \rho \mathcal{C} h, \tag{2.38}$$

where $h \in \mathbb{R}^6$, $\mathcal{C} \in \mathbb{R}^{6\times 6}$, and $\mathcal{D} \in \mathbb{R}^{6\times 6}$ are given by

$$h = \begin{pmatrix} f^0 \\ \tau^0 \end{pmatrix}, \quad \mathcal{C} = \mathcal{M} \Lambda^T \mathbb{Q}^T, \quad \mathcal{D} = k\Theta \mathcal{M}. \tag{2.39}$$

Partitioned forms of $\mathcal{C}$ and $\mathcal{D}$ (or $\mathcal{M}$) are given in (2.30) and (2.29). Eliminating J between (2.38) and (2.37) yields

$$\frac{\partial \rho}{\partial t} = g^{-1} \nabla \cdot (g\mathcal{D} \nabla \rho - g\rho \mathcal{C} h), \quad (q, \eta) \in \mathcal{E} \times \mathcal{A}, \quad t > 0. \tag{2.40}$$

Equation (2.40) is a linear, variable-coefficient, convection-diffusion equation which describes the evolution of the particle density ρ, defined per unit volume of the intrinsic configuration space, under arbitrary external loads. It is expected to be valid only for dilute solutions in which the solute particles are identical, well separated, and small compared to the size of the domain occupied by the solution. While this

equation describes the evolution of the density in the local coordinate space $\mathcal{E} \times \mathcal{A}$ and hence depends on the choice of the coordinate chart Φ, we remark that the induced evolution on the intrinsic configuration space $\mathrm{E} \times \mathrm{SO}_3$ is independent of this choice. Indeed, (2.40) can be interpreted as the local representation of a convection-diffusion equation on $\mathrm{E} \times \mathrm{SO}_3$. This equation seems to have first appeared in work by Brenner [4, 5], where it was derived by a different approach.

Aside from geometric factors associated with the local coordinate chart and physical constants, the convection and diffusion matrices $\mathcal{C}$ and $\mathcal{D}$ appearing in (2.40) are entirely determined by the shape of a solute particle through the hydrodynamic mobility matrix M, or its local representation $\mathcal{M}$. The diagonal blocks $\mathcal{C}_1, \mathcal{D}_1 \in \mathbb{R}^{3\times 3}$ are associated with the translational motion of a particle, whereas $\mathcal{C}_4, \mathcal{D}_4 \in \mathbb{R}^{3\times 3}$ are associated with rotational motion. The off-diagonal blocks $\mathcal{C}_{2,3}, \mathcal{D}_{2,3} \in \mathbb{R}^{3\times 3}$ are associated with cross-coupling between translational and rotational motion, whereas the off-diagonal entries in the diagonal blocks $\mathcal{C}_{1,4}, \mathcal{D}_{1,4} \in \mathbb{R}^{3\times 3}$ are associated with self-coupling. The relation $\mathcal{D} = k\Theta\mathcal{M}$ between the diffusion and mobility matrices can be viewed as a generalization, to a particle of arbitrary shape, of the classic Stokes–Einstein relation for a particle of spherical or ellipsoidal shape [7, 10, 25].

3. Analysis. Here we outline an initial-boundary value problem for the diffusion of rigid particles in a viscous solvent, transform it into a dimensionless form convenient for analysis, and use perturbation techniques to derive leading-order equations for the particle dynamics at different time scales. We show that the leading-order equations are characterized by scalar coefficients with simple interpretations and study their properties.

3.1. Initial-boundary value problem. To state an initial-boundary value problem for the density field ρ, it is first necessary to consider appropriate boundary conditions for (2.40). To this end, we view this equation as the local representation of an equation on $\mathrm{E} \times \mathrm{SO}_3$ and note that, since SO_3 has no boundary, $\partial(\mathrm{E} \times \mathrm{SO}_3) = \partial\mathrm{E} \times \mathrm{SO}_3$. Thus the only intrinsic boundary conditions are those pertaining to the physical domain E which contains the solvent and solute particles. Assuming that the boundary of E is impermeable, we require that the normal component of the intrinsic mass flux vanish on $\partial\mathrm{E} \times \mathrm{SO}_3$. In terms of a coordinate chart on $\mathcal{E} \times \mathcal{A}$, the representation of this condition is

$$gJ \cdot \nu = 0, \quad (q, \eta) \in \partial\mathcal{E} \times \mathcal{A}, \tag{3.1}$$

where ν is the outward unit normal on $\partial(\mathcal{E} \times \mathcal{A}) = (\partial\mathcal{E} \times \mathcal{A}) \cup (\mathcal{E} \times \partial\mathcal{A})$. Notice that $\nu = (\nu_q, 0)$ on $\partial\mathcal{E} \times \mathcal{A}$ and $\nu = (0, \nu_\eta)$ on $\mathcal{E} \times \partial\mathcal{A}$, where ν_q and ν_η are the outward unit normals on $\partial\mathcal{E}$ and $\partial\mathcal{A}$.

Special considerations are required on the boundary component $\mathcal{E} \times \partial\mathcal{A}$, which has no intrinsic counterpart and is entirely associated with the coordinate chart Φ. Without loss of generality, we consider charts based on standard Euler angle parameterizations of SO_3, for which $\mathcal{A}$ is the Cartesian product of open intervals $\mathcal{I}_i = (a_i, b_i)$, where each coordinate η_i is either regular or singular in the sense that $g \neq 0$ or $g = 0$ on $\partial\mathcal{I}_i$. For such charts, the local representation of any function on SO_3 is periodic in the regular coordinates. Because of this periodicity, and the fact that the outward normals on opposite faces of $\partial\mathcal{A}$ are oppositely oriented, we find that an appropriate boundary condition on the normal component of the mass flux is, for each i,

$$gJ \cdot \nu|_{\eta_i = b_i} = -gJ \cdot \nu|_{\eta_i = a_i}, \quad (q, \eta_i') \in \mathcal{E} \times \partial'\mathcal{A}_i. \tag{3.2}$$

Here $\partial'\mathcal{A}_i = \mathcal{I}_j \times \mathcal{I}_k$ and $\eta_i' = (\eta_j, \eta_k)$, where $j < k$ are indices distinct from i. Notice that (3.2) implies periodicity when $g \neq 0$ and is trivially satisfied when $g = 0$ on $\partial\mathcal{I}_i$.

An initial-boundary value problem for the diffusion of rigid particles of arbitrary shape in a viscous solvent can now be stated. Combining (2.38)–(3.2) we find that, for a given initial condition ρ_0, the time-dependent particle density field $\rho : \mathcal{E} \times \mathcal{A} \times [0,\infty) \to \mathbb{R}$ must satisfy

$$
\begin{aligned}
&\frac{\partial}{\partial t}\rho = g^{-1}\nabla\cdot(g\mathcal{D}\nabla\rho - g\rho\mathcal{C}h), && (q,\eta) \in \mathcal{E}\times\mathcal{A}, && t > 0,\\
&g(\mathcal{D}\nabla\rho - \rho\mathcal{C}h)\cdot\nu = 0, && (q,\eta) \in \partial\mathcal{E}\times\mathcal{A}, && t \geq 0,\\
&\sum_{\eta_i\in\partial\mathcal{I}_i} g(\mathcal{D}\nabla\rho - \rho\mathcal{C}h)\cdot\nu = 0, && (q,\eta_i') \in \mathcal{E}\times\partial'\mathcal{A}_i, && t \geq 0,\\
&\rho|_{t=0} = \rho_0, && (q,\eta) \in \mathcal{E}\times\mathcal{A}, && t = 0.
\end{aligned}
\tag{3.3}
$$

3.2. Nondimensionalization. Here we introduce various scales relevant to (3.3) and transform it into a dimensionless form convenient for analysis. We first introduce the projection matrices $P_q, P_\eta \in \mathbb{R}^{6\times 6}$ defined in partitioned form by

$$
P_q = \begin{pmatrix} 1 & 0 \\ 0 & 0 \end{pmatrix}, \quad P_\eta = \begin{pmatrix} 0 & 0 \\ 0 & 1 \end{pmatrix},
\tag{3.4}
$$

where $0, 1 \in \mathbb{R}^{3\times 3}$ denote the zero and identity matrices. For any scalars a, b we notice that the matrix $(aP_q + bP_\eta)$ is symmetric and commutes with any block-diagonal matrix, and moreover, if $a, b \neq 0$, then it is invertible with inverse $(a^{-1}P_q + b^{-1}P_\eta)$. Furthermore, for any scalars a, b, c, d we have $(aP_q + bP_\eta)(cP_q + dP_\eta) = (acP_q + bdP_\eta)$.

To define dimensionless quantities associated with the space of admissible configurations, we introduce a characteristic length scale L for the spatial domain E and define dimensionless variables by

$$
r^* = L^{-1}r, \quad Q^* = Q, \quad q^* = q, \quad \eta^* = \eta,
\tag{3.5}
$$

where, without loss of generality, we assume that the local coordinates are dimensionless. The above definitions imply a dimensionless coordinate chart $\Phi^* = (\psi^*, \phi^*) : \mathcal{E}^* \times \mathcal{A}^* \to \mathrm{E}^* \times \mathrm{SO}_3^*$, where $\psi^* = L^{-1}\psi$ and $\phi^* = \phi$. From (2.33) we deduce the dimensionless Jacobian factors $g^* = L^{-3}g$, $g^*_{q^*} = L^{-3}g_q$, and $g^*_{\eta^*} = g_\eta$, and from (2.22) and (2.20) we deduce the dimensionless connection matrix

$$
\Lambda^* = (L^{-1}P_q + P_\eta)\Lambda = \Lambda(L^{-1}P_q + P_\eta),
\tag{3.6}
$$

where the second equality follows from the fact that Λ is block diagonal. Moreover, from (2.12) we deduce $\mathbb{Q}^* = \mathbb{Q}$.

To define dimensionless quantities associated with an individual solute particle, we introduce a characteristic length scale ℓ for the particle and force scale α for the external loads. We then define dimensionless mobility matrices by

$$
\begin{aligned}
M_1^* &= \mu\ell M_1, \quad M_2^* = \mu\ell^2 M_2,\\
M_3^* &= \mu\ell^2 M_3, \quad M_4^* = \mu\ell^3 M_4,
\end{aligned}
\tag{3.7}
$$

where μ is the absolute viscosity of the solvent, and dimensionless external loads by

$$
f^{0*} = \alpha^{-1}f^0, \quad \tau^{0*} = \alpha^{-1}\ell^{-1}\tau^0.
\tag{3.8}
$$

The scaling of the mobility matrices in (3.7) and the torque in (3.8) is consistent with a standard Stokesian hydrodynamic model and the relation between force and torque for a particle of characteristic size ℓ. Expressing these component relations in matrix form, we get

$$\begin{aligned} M^* &= \mu\ell(P_q + \ell P_\eta)M(P_q + \ell P_\eta), \\ h^* &= \alpha^{-1}(P_q + \ell^{-1}P_\eta)h. \end{aligned} \tag{3.9}$$

A dimensionless form of the initial-boundary value problem can now be stated. Let t_c be an arbitrary time scale, let ρ_c be an arbitrary density scale, and introduce the dimensionless variables $t^* = t_c^{-1}t$ and $\rho^* = \rho_c^{-1}\rho$. Then a dimensionless form of (3.3) is given by (using flux notation for convenience)

$$\begin{aligned} &\frac{\partial}{\partial t^*}\rho^* + (g^*)^{-1}\nabla^* \cdot (g^* J^*) = 0, && (q^*, \eta^*) \in \mathcal{E}^* \times \mathcal{A}^*, && t^* > 0, \\ &g^* J^* \cdot \nu^* = 0, && (q^*, \eta^*) \in \partial\mathcal{E}^* \times \mathcal{A}^*, && t^* \geq 0, \\ &\sum_{\eta_i^* \in \partial\mathcal{I}_i^*} g^* J^* \cdot \nu^* = 0, && (q^*, \eta_i^{*\prime}) \in \mathcal{E}^* \times \partial'\mathcal{A}_i^*, && t^* \geq 0, \\ &\rho^*|_{t^*=0} = \rho_0^*, && (q^*, \eta^*) \in \mathcal{E}^* \times \mathcal{A}^*, && t^* = 0. \end{aligned} \tag{3.10}$$

Here $\nabla^* = (\nabla_{q^*}, \nabla_{\eta^*})$ is the gradient with respect to the coordinates (q^*, η^*), ν^* is the outward unit normal on the boundary of $\mathcal{E}^* \times \mathcal{A}^*$, $J^* = -\mathcal{D}^*\nabla^*\rho^* + \rho^*\mathcal{C}^*h^*$ is a dimensionless mass flux, $\mathcal{C}^*, \mathcal{D}^*$ are dimensionless convection and diffusion matrices defined by

$$\begin{aligned} \mathcal{C}^* &= (aP_q + bP_\eta)\mathcal{M}^*\Lambda^{*T}\mathbb{Q}^{*T}, \\ \mathcal{D}^* &= (cP_q + dP_\eta)\mathcal{M}^*(cP_q + dP_\eta), \end{aligned} \tag{3.11}$$

$\mathcal{M}^* = (\Lambda^*)^{-1}M^*(\Lambda^*)^{-T}$ is a dimensionless mobility matrix, and a, b, c, d are dimensionless parameters defined by

$$a = \frac{\alpha t_c}{\mu\ell L}, \quad b = \frac{\alpha t_c}{\mu\ell^2}, \quad c = \sqrt{\frac{k\Theta t_c}{\mu\ell L^2}}, \quad d = \sqrt{\frac{k\Theta t_c}{\mu\ell^3}}. \tag{3.12}$$

3.3. Scaling limits. Here we use perturbation techniques [22, 41] on (3.10) to derive leading-order equations for the particle dynamics at different time scales. We restrict our attention to the dimensionless formulation outlined above and omit the superscript stars for brevity. We consider three basic scales corresponding to translational diffusion, translational sedimentation, and rotational diffusion. In the latter case, we consider the rotational diffusion of not only the particle-fixed frame, but also of a single, arbitrary particle-fixed vector.

Translational diffusion scale. We consider the dynamics of particles on the time scale $t_{c,\mathrm{t}} = \mu\ell L^2/k\Theta$. This scale is based on the classic theory of diffusion of spherical particles [7, 10, 37]. Up to a multiplicative constant, it is the time required for a particle of size ℓ to translate a distance L by diffusion (Brownian motion) in a solvent of viscosity μ at temperature Θ. Substituting this time scale into (3.12) and (3.11), we get

$$\begin{aligned} \mathcal{C} &= \delta\left(P_q + \frac{1}{\epsilon}P_\eta\right)\mathcal{M}\Lambda^T\mathbb{Q}^T, \\ \mathcal{D} &= \left(P_q + \frac{1}{\epsilon}P_\eta\right)\mathcal{M}\left(P_q + \frac{1}{\epsilon}P_\eta\right), \end{aligned} \tag{3.13}$$

where $\epsilon = \ell/L$ is the ratio of particle size to diffusion distance and $\delta = \alpha L/k\Theta$ is the ratio of external potential energy to thermal energy of a particle.

Assuming $\epsilon \ll 1$, we can derive a leading-order approximation of (3.10). Indeed, in view of (3.13), we find that the system is singularly perturbed. Away from an initial layer in time, the leading-order equations are

$$\begin{aligned} &\nabla_\eta \cdot (g_\eta \mathcal{D}_4 \nabla_\eta \rho) = 0, \qquad (q,\eta) \in \mathcal{E} \times \mathcal{A}, \qquad t > 0, \\ &\sum_{\eta_i \in \partial \mathcal{J}_i} g_\eta \mathcal{D}_4 \nabla_\eta \rho \cdot \nu_\eta = 0, \quad (q,\eta_i') \in \mathcal{E} \times \partial' \mathcal{A}_i, \quad t > 0. \end{aligned} \tag{3.14}$$

Multiplying the first relation in (3.14) by ρ, integrating over $\mathcal{A}$, and then using the second relation together with the positivity of g_η and $\mathcal{D}_4$, we deduce that $\nabla_\eta \rho = 0$ in $\mathcal{E} \times \mathcal{A}$. This implies that ρ is independent of the coordinates η, or equivalently that $\rho = \mathbb{P}\rho$, where $\mathbb{P}$ is a projection operator defined for any function $f : \mathcal{E} \times \mathcal{A} \to \mathbb{R}$ by

$$\mathbb{P} f = \frac{\int_{\mathcal{A}} f \, dV_\eta}{\int_{\mathcal{A}} dV_\eta}. \tag{3.15}$$

An evolution equation for the projection $\mathbb{P}\rho$, or any multiple of it, away from an initial layer in time can also be deduced. Specifically, multiplying the first relation in (3.10) by g_η, applying the operator $\mathbb{P}$ to this relation and the second, and then using the third relation and the fact that ρ is independent of η, or equivalently that $\rho = \mathbb{P}\rho$, we obtain

$$\begin{aligned} &\frac{\partial}{\partial t}\rho_{\mathrm{t}} = g_q^{-1} \nabla_q \cdot (g_q \widehat{\mathcal{D}}_1 \nabla_q \rho_{\mathrm{t}} - g_q \rho_{\mathrm{t}} \widehat{\gamma}), \quad q \in \mathcal{E}, \qquad t > 0, \\ &g_q (\widehat{\mathcal{D}}_1 \nabla_q \rho_{\mathrm{t}} - \rho_{\mathrm{t}} \widehat{\gamma}) \cdot \nu_q = 0, \qquad\qquad q \in \partial\mathcal{E}, \quad t > 0, \end{aligned} \tag{3.16}$$

where ρ_{t} is the particle density per unit volume of the spatial domain E defined by

$$\rho_{\mathrm{t}} = \int_{\mathcal{A}} \rho g_\eta \, dV_\eta, \tag{3.17}$$

and $\widehat{\mathcal{D}}_1 \in \mathbb{R}^{3\times 3}$ and $\widehat{\gamma} \in \mathbb{R}^3$ are defined by

$$\widehat{\mathcal{D}}_1 = \frac{\mathbb{P}(g_\eta \mathcal{D}_1)}{\mathbb{P} g_\eta}, \quad \widehat{\gamma} = \frac{\mathbb{P}(g_\eta \mathcal{C}_1 f^0 + g_\eta \mathcal{C}_3 \tau^0)}{\mathbb{P} g_\eta}. \tag{3.18}$$

From the definition of the projection $\mathbb{P}$ and the Jacobian factor g_η, we deduce that $\widehat{\mathcal{D}}_1$ and $\widehat{\gamma}$ can be interpreted as the averages of $\mathcal{D}_1$ and $\mathcal{C}_1 f^0 + \mathcal{C}_3 \tau^0$ over the space SO_3 of particle orientations. Assuming the external load components (f^0, τ^0) are independent of the particle orientation coordinates η, we can evaluate both averages in (3.18) explicitly. Working in any local coordinates for SO_3, for example, the Euler angle chart introduced later, we find from (3.13) that

$$\widehat{\mathcal{D}}_1 = \mathcal{D}_{\mathrm{t}} \, \nabla_q \psi^{-1} \nabla_q \psi^{-T}, \quad \widehat{\gamma} = \delta \, \nabla_q \psi^{-1} (\mathcal{D}_{\mathrm{t}} f^0 + \mathcal{D}_{\mathrm{tr}} \tau^0), \tag{3.19}$$

where $\mathcal{D}_{\mathrm{t}} > 0$ and $\mathcal{D}_{\mathrm{tr}}$ are constant scalar coefficients given by

$$\mathcal{D}_{\mathrm{t}} = \frac{1}{3} \operatorname{tr}(M_1), \quad \mathcal{D}_{\mathrm{tr}} = \frac{1}{3} \operatorname{tr}(M_3). \tag{3.20}$$

Notice that $\mathcal{D}_{\mathrm{t}}$ is the orientational average of the matrix M_1 associated with pure translational motion, and $\mathcal{D}_{\mathrm{tr}}$ is the orientational average of the matrix M_3 associated with cross-coupling between translational and rotational motion.

The system defined by (3.16)–(3.18) and (3.19) takes a particularly simple form when the local coordinates q are Cartesian and there are no external loads. In this case, $\mathcal{E}$ is identified with E, $\nabla_q\psi$ is the identity, g_q is unity, and $\widehat{\gamma}$ is zero, and we obtain

$$\begin{aligned} &\frac{\partial}{\partial t}\rho_{\mathrm{t}} = \mathcal{D}_{\mathrm{t}}\Delta_q\rho_{\mathrm{t}}, \quad q \in \mathrm{E}, \qquad t > 0, \\ &\mathcal{D}_{\mathrm{t}}\nabla_q\rho_{\mathrm{t}} \cdot \nu_q = 0, \quad q \in \partial\mathrm{E}, \quad t > 0. \end{aligned} \tag{3.21}$$

This is an isotropic diffusion equation for the ordinary particle density ρ_{t}. It is a leading-order approximation of (3.10) on the translational diffusion time scale $t_{c,\mathrm{t}}$ under the assumption that ϵ is small. It shows that, regardless of the details of the particle geometry and the cross- and self-coupling effects reflected in the hydrodynamic mobility matrix M, the translational motion of particles is decoupled from rotational motion at this time scale and is characterized to leading order by the scalar translational diffusion coefficient $\mathcal{D}_{\mathrm{t}}$. Moreover, from (3.16)–(3.20) we deduce that the influence of an orientation-independent external load f^0 is also characterized by the translational coefficient $\mathcal{D}_{\mathrm{t}}$, whereas the influence of an orientation-independent external torque τ^0 is characterized by the coupling coefficient $\mathcal{D}_{\mathrm{tr}}$.

Translational sedimentation scale. We consider the dynamics of particles on the time scale $t_{c,\mathrm{s}} = \mu\ell L/\alpha$. This scale is based on the classic theory of sedimentation of spherical particles [7, 14, 37]. Up to a multiplicative constant, it is the time required for a particle of size ℓ to translate a distance L by sedimentation under a force of magnitude α in a solvent of viscosity μ. Substituting this time scale into (3.12) and (3.11), we get

$$\begin{aligned} \mathcal{C} &= \left(P_q + \frac{1}{\epsilon}P_\eta\right)\mathcal{M}\Lambda^T\mathbb{Q}^T, \\ \mathcal{D} &= \lambda\left(P_q + \frac{1}{\epsilon}P_\eta\right)\mathcal{M}\left(P_q + \frac{1}{\epsilon}P_\eta\right), \end{aligned} \tag{3.22}$$

where $\epsilon = \ell/L$ is the ratio of particle size to sedimentation distance and $\lambda = k\Theta/\alpha L$ is the ratio of thermal energy to external potential energy of a particle.

Assuming $\epsilon \ll 1$, the system in (3.10) is singularly perturbed with the same structure as before, and we again arrive at the leading-order approximation given in (3.16)–(3.18). Moreover, assuming that the external loads (f^0, τ^0) are due solely to centrifugal and uniform body force effects, so that f^0 is independent of η, and τ^0 depends on η only through the particle inertia matrix in the centrifugal term, we can evaluate both averages in (3.18) explicitly. Indeed, the contributions of the external torque vanish, and we obtain

$$\widehat{\mathcal{D}}_1 = \lambda\mathcal{D}_{\mathrm{t}}\,\nabla_q\psi^{-1}\nabla_q\psi^{-T}, \quad \widehat{\gamma} = \mathcal{D}_{\mathrm{t}}\nabla_q\psi^{-1}f^0, \tag{3.23}$$

where $\mathcal{D}_{\mathrm{t}} > 0$ is the translational diffusion coefficient defined in (3.20).

The system defined by (3.16)–(3.18) and (3.23) takes a particularly simple form when the local coordinates q are Cartesian. As before, $\mathcal{E}$ is identified with E, $\nabla_q\psi$ is

the identity, and g_q is unity, and we obtain

$$\begin{aligned} &\frac{\partial}{\partial t}\rho_{\mathrm{t}} = \nabla_q \cdot (\lambda \mathcal{D}_{\mathrm{t}} \nabla_q \rho_{\mathrm{t}} - \mathcal{D}_{\mathrm{t}} \rho_{\mathrm{t}} f^0), && q \in \mathrm{E}, \quad t > 0, \\ &(\lambda \mathcal{D}_{\mathrm{t}} \nabla_q \rho_{\mathrm{t}} - \mathcal{D}_{\mathrm{t}} \rho_{\mathrm{t}} f^0) \cdot \nu_q = 0, && q \in \partial\mathrm{E}, \quad t > 0. \end{aligned} \tag{3.24}$$

This equation can be recognized as the classic Lamm equation [7, 14, 37] written in Cartesian coordinates with dimensionless sedimentation coefficient equal to $\mathcal{D}_{\mathrm{t}}$. This equation is a leading-order approximation of (3.10) on the translational sedimentation time scale $t_{c,\mathrm{s}}$ under the assumption that ϵ is small. As before, it shows that, regardless of the details of the particle geometry and the cross- and self-coupling effects reflected in the hydrodynamic mobility matrix M, the translational motion of particles is decoupled from rotational motion at this time scale and is characterized to leading order by the scalar translational diffusion coefficient $\mathcal{D}_{\mathrm{t}}$.

Rotational diffusion scale. We consider the dynamics of particles on the time scale $t_{c,\mathrm{r}} = \mu\ell^3/k\Theta$. This scale is based on the classic theory of rotational diffusion of ellipsoidal particles [7, 30, 31, 37]. Up to a multiplicative constant, it is the time required for a particle of size ℓ to rotate through a unit radian angle by diffusion in a solvent of viscosity μ at temperature Θ. Substituting this time scale into (3.12) and (3.11), we get

$$\begin{aligned} \mathcal{C} &= \delta\epsilon(\epsilon P_q + P_\eta)\mathcal{M}\Lambda^T\mathbb{Q}^T, \\ \mathcal{D} &= (\epsilon P_q + P_\eta)\mathcal{M}(\epsilon P_q + P_\eta), \end{aligned} \tag{3.25}$$

where $\epsilon = \ell/L$ and $\delta = \alpha L/k\Theta$ are parameters as defined before.

Assuming $\epsilon \ll 1$, we can again derive a leading-order approximation of (3.10), which in contrast to the previous two cases is now regularly perturbed. Indeed, substituting (3.25) into (3.10), retaining only the leading-order terms, multiplying by g_q, and then integrating over $\mathcal{E}$, we obtain

$$\begin{aligned} &\frac{\partial}{\partial t}\rho_{\mathrm{r}} = g_\eta^{-1}\nabla_\eta \cdot (g_\eta \mathcal{D}_4 \nabla_\eta \rho_{\mathrm{r}}), && \eta \in \mathcal{A}, && t > 0, \\ &\sum_{\eta_i \in \partial\mathcal{J}_i} g_\eta \mathcal{D}_4 \nabla_\eta \rho_{\mathrm{r}} \cdot \nu_\eta = 0, && \eta_i' \in \partial'\mathcal{A}_i, && t \geq 0, \\ &\rho_{\mathrm{r}}|_{t=0} = \rho_{\mathrm{r}0}, && \eta \in \mathcal{A}, && t = 0, \end{aligned} \tag{3.26}$$

where ρ_{r} is the particle density per unit volume of SO_3 defined by

$$\rho_{\mathrm{r}} = \int_{\mathcal{E}} \rho g_q \, dV_q. \tag{3.27}$$

This is a local representation of a diffusion equation on the manifold SO_3. It is a leading-order approximation of (3.10) on the rotational diffusion time scale $t_{c,\mathrm{r}}$ under the assumption that ϵ is small. It shows that, regardless of the details of the particle geometry and the cross-coupling effects reflected in the hydrodynamic mobility matrix M, the rotational motion of particles is decoupled from translational motion at this time scale and is characterized to leading order by the rotational diffusion block $\mathcal{D}_4 \in \mathbb{R}^{3\times3}$. Notice that, whereas cross-coupling effects vanish, self-coupling effects may still be present as reflected in the off-diagonal entries of $\mathcal{D}_4$.

Rotational diffusion of a single vector. In some applications, the motion of a single unit vector $\boldsymbol{n}$ fixed in each particle, and not the three orthonormal frame vectors $\{\boldsymbol{d}_i\}$, is of primary interest. Here we study the dynamics of a single unit vector on the rotational time scale introduced above. For simplicity, we initially assume that the given unit vector $\boldsymbol{n}$ of interest corresponds to the particle frame vector $\boldsymbol{d}_3$. This can always be achieved by a suitable rotation of the particle frame. Let $M_4 \in \mathbb{R}^{3\times 3}$ be the rotational block of the hydrodynamic mobility matrix in the particle frame, and define constant scalar coefficients $\mathcal{D}_{\mathrm{r}}^{\perp} > 0$ and $\mathcal{D}_{\mathrm{r}}^{\parallel} > 0$ associated with rotation transverse and parallel to $\boldsymbol{d}_3$ by

$$\mathcal{D}_{\mathrm{r}}^{\perp} = \frac{M_4^{11} + M_4^{22}}{2}, \quad \mathcal{D}_{\mathrm{r}}^{\parallel} = M_4^{33}. \tag{3.28}$$

From (3.25) we have $\mathcal{D}_4 = \mathcal{M}_4 = S^{-1} M_4 S^{-T}$, and by definition of $\mathcal{D}_{\mathrm{r}}^{\perp}$ and $\mathcal{D}_{\mathrm{r}}^{\parallel}$ we can write

$$\mathcal{D}_4 = S^{-1}(\mathcal{D}_{\mathrm{r}}^{\perp} M_4^{\perp} + \mathcal{D}_{\mathrm{r}}^{\parallel} M_4^{\parallel}) S^{-T}, \tag{3.29}$$

where $M_4^{\perp} \in \mathbb{R}^{3\times 3}$ and $M_4^{\parallel} \in \mathbb{R}^{3\times 3}$ are scaled matrices defined by

$$M_4^{\perp} = \frac{1}{\mathcal{D}_{\mathrm{r}}^{\perp}} \begin{pmatrix} M_4^{11} & M_4^{12} & M_4^{13} \\ M_4^{21} & M_4^{22} & M_4^{23} \\ M_4^{31} & M_4^{32} & 0 \end{pmatrix}, \quad M_4^{\parallel} = \begin{pmatrix} 0 & 0 & 0 \\ 0 & 0 & 0 \\ 0 & 0 & 1 \end{pmatrix}. \tag{3.30}$$

We consider a system of Euler angle coordinates $\eta = (\eta_1, \eta_2, \eta_3)$ on SO_3 in which η_2 and η_3 are the latitudinal and longitudinal coordinates of $\boldsymbol{d}_3$ on the unit sphere, and η_1 is a twist coordinate which locates $\boldsymbol{d}_1$ and $\boldsymbol{d}_2$ in the tangent plane to the sphere at $\boldsymbol{d}_3$ as illustrated in Figure 3.1. Specifically, we consider the Euler angle chart $\phi : \mathcal{A} \to \mathrm{SO}_3$ defined by [17, 23]

$$\phi = \begin{pmatrix} c_1c_3 - c_2s_1s_3 & -c_3s_1 - c_1c_2s_3 & s_2s_3 \\ c_2c_3s_1 + c_1s_3 & c_1c_2c_3 - s_1s_3 & -c_3s_2 \\ s_1s_2 & c_1s_2 & c_2 \end{pmatrix}, \tag{3.31}$$

where $c_i = \cos(\eta_i)$, $s_i = \sin(\eta_i)$, and $\mathcal{A} = (0, 2\pi) \times (0, \pi) \times (0, 2\pi)$. For this chart, the associated Jacobian factor is $g_\eta = 2\sqrt{2}\sin\eta_2$ and the associated structure matrix $S \in \mathbb{R}^{3\times 3}$ and its inverse are

$$S = \begin{pmatrix} 0 & c_1 & s_1s_2 \\ 0 & -s_1 & c_1s_2 \\ 1 & 0 & c_2 \end{pmatrix}, \quad S^{-1} = \begin{pmatrix} -\frac{c_2s_1}{s_2} & -\frac{c_1c_2}{s_2} & 1 \\ c_1 & -s_1 & 0 \\ \frac{s_1}{s_2} & \frac{c_1}{s_2} & 0 \end{pmatrix}. \tag{3.32}$$

Assuming $M_4^{\perp}$ is of order unity and that $\mathcal{D}_{\mathrm{r}}^{\parallel} \gg \mathcal{D}_{\mathrm{r}}^{\perp}$, we can derive a leading-order approximation of (3.26). Indeed, in view of (3.29), we find that the system is singularly perturbed. Away from an initial layer in time, the leading-order equations are

$$\begin{aligned} &\frac{\partial}{\partial\eta_1}\left(\mathcal{D}_{\mathrm{r}}^{\parallel}\frac{\partial}{\partial\eta_1}\rho_{\mathrm{r}}\right) = 0, \quad \eta \in \mathcal{A}, \qquad t > 0, \\ &\mathcal{D}_{\mathrm{r}}^{\parallel}\frac{\partial}{\partial\eta_1}\rho_{\mathrm{r}}|_{\eta_1=0}^{\eta_1=2\pi} = 0, \qquad \eta_1' \in \partial'\mathcal{A}_1, \quad t > 0. \end{aligned} \tag{3.33}$$

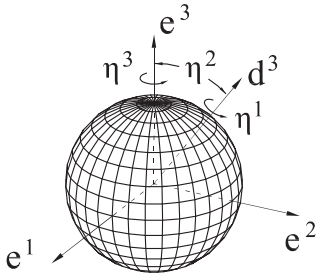

FIG. 3.1. *Illustration of Euler angle coordinates for the orientation of the particle frame* $\{\boldsymbol{d}_i\}$ *relative to the experimental frame* $\{\boldsymbol{e}_i\}$. η_2 *and* η_3 *are the coordinates of* $\boldsymbol{d}_3$ *on the unit sphere, and* η_1 *is a twist coordinate which locates* $\boldsymbol{d}_1$ *and* $\boldsymbol{d}_2$ *(not shown) in the tangent plane to the sphere at* $\boldsymbol{d}_3$.

Multiplying the first relation in (3.33) by ρ_{r}, integrating over η_1, and then using the second relation together with the positivity of $\mathcal{D}_{\mathrm{r}}^{\parallel}$, we deduce that $\partial\rho_{\mathrm{r}}/\partial\eta_1 = 0$ in $\mathcal{A}$. This implies that ρ_{r} is independent of the coordinate η_1, or equivalently that $\rho_{\mathrm{r}} = \mathbb{A}\rho_{\mathrm{r}}$, where $\mathbb{A}$ is a projection operator defined for any function $f : \mathcal{A} \to \mathbb{R}$ by

$$\mathbb{A}f = \frac{1}{2\pi}\int_0^{2\pi} f \, d\eta_1. \tag{3.34}$$

Just as in the translational case, an evolution equation for the projected density away from an initial layer in time can be deduced. Specifically, applying the operator $\mathbb{A}$ to the first relation and the last two components of the second relation in (3.26), and using the fact that ρ_{r} is independent of η_1, or equivalently that $\rho_{\mathrm{r}} = \mathbb{A}\rho_{\mathrm{r}}$, we obtain

$$\begin{aligned} &\frac{\partial}{\partial t}\rho_{\mathrm{d}_3} = g_\sigma^{-1}\nabla_\sigma \cdot (g_\sigma \widehat{\mathcal{D}}_4 \nabla_\sigma \rho_{\mathrm{d}_3}), \quad \sigma \in \mathcal{S}, \qquad t > 0, \\ &\sum_{\sigma_i \in \partial\mathcal{K}_i} g_\sigma \widehat{\mathcal{D}}_4 \nabla_\sigma \rho_{\mathrm{d}_3} \cdot \nu_\sigma = 0, \qquad \sigma_i' \in \partial'\mathcal{S}_i, \quad t > 0, \end{aligned} \tag{3.35}$$

where $\sigma = (\eta_2, \eta_3)$ are coordinates on the unit sphere, $\mathcal{K}_1 = (0, \pi)$ is the domain of σ_1, $\mathcal{K}_2 = (0, 2\pi)$ is the domain of σ_2, and $\mathcal{S} = \mathcal{K}_1 \times \mathcal{K}_2$, $\partial'\mathcal{S}_i = \mathcal{K}_j$, $\sigma_i' = \sigma_j$ $(i = 1, 2;$ $j \neq i)$ is notation analogous to before. In the above equation, $g_\sigma = \sin\eta_2$ is the associated Jacobian factor, ν_σ is the outward unit normal on $\partial\mathcal{S}$, ρ_{d_3} is the particle density per unit area of the unit sphere defined by

$$\rho_{\mathrm{d}_3} = \int_0^{2\pi} \rho_{\mathrm{r}} \, d\eta_1, \tag{3.36}$$

and $\widehat{\mathcal{D}}_4 \in \mathbb{R}^{2\times 2}$ is the average over the twist coordinate η_1 of the projection of $\mathcal{D}_4$ onto the two-dimensional coordinate space corresponding to η_2 and η_3, namely,

$$\widehat{\mathcal{D}}_4 = \mathbb{A}(\mathcal{P}\mathcal{D}_4\mathcal{P}^T), \quad \mathcal{P} = \begin{pmatrix} 0 & 1 & 0 \\ 0 & 0 & 1 \end{pmatrix}, \tag{3.37}$$

where $\mathcal{P} \in \mathbb{R}^{2\times 3}$ is the coordinate projection matrix. The average in the above equation can be computed explicitly. Indeed, if $\mathcal{D}_{\mathrm{r}}^{\perp}$ is the transverse rotational diffusion coefficient defined in (3.28), then

$$\widehat{\mathcal{D}}_4 = \mathcal{D}_{\mathrm{r}}^{\perp} \begin{pmatrix} 1 & 0 \\ 0 & 1/\sin^2\eta_2 \end{pmatrix}. \tag{3.38}$$

The system defined by (3.35)–(3.38) can be identified as a local representation of an isotropic diffusion equation on the unit sphere. It is a leading-order approximation of (3.26) under the assumption that the hydrodynamic ratio $\mathcal{D}_{\mathrm{r}}^{\perp}/\mathcal{D}_{\mathrm{r}}^{\parallel}$ is small. It shows that, regardless of the self-coupling effects reflected in the rotational diffusion block $\mathcal{D}_4$, the motion of the single unit vector $\boldsymbol{d}_3$ is described by an isotropic equation and is characterized to leading order by the scalar coefficient $\mathcal{D}_{\mathrm{r}}^{\perp}$. We remark that when ρ_{d_3} can be approximated as being uniform in the angle η_3 (see Figure 3.1), the system defined by (3.35)–(3.38) can be further reduced to a one-dimensional, axisymmetric equation on the sphere.

The above results also apply when the unit vector of interest is not $\boldsymbol{d}_3$, but rather a given unit vector $\boldsymbol{n}$. Indeed, if we let η_2 and η_3 be the latitudinal and longitudinal coordinates of $\boldsymbol{n}$ relative to the experimental frame, then the motion of $\boldsymbol{n}$ is described to leading order by an isotropic diffusion equation of the same form as above with coefficient $\mathcal{D}_{\mathrm{r},n}^{\perp}$, provided the ratio $\mathcal{D}_{\mathrm{r},n}^{\perp}/\mathcal{D}_{\mathrm{r},n}^{\parallel}$ is small, where

$$\mathcal{D}_{\mathrm{r},n}^{\perp} = \frac{1}{2}\operatorname{tr}(P_n M_4 P_n), \quad \mathcal{D}_{\mathrm{r},n}^{\parallel} = n \cdot M_4 n. \tag{3.39}$$

Here $n \in \mathbb{R}^3$ are components in the particle frame and $P_n = I - nn^T \in \mathbb{R}^{3\times 3}$ is the projection onto the two-dimensional subspace orthogonal to n. Notice that the relations in (3.39) reduce to those in (3.28) when $n = (0, 0, 1)$, equivalently $\boldsymbol{n} = \boldsymbol{d}_3$, and that $\mathcal{D}_{\mathrm{r},n}^{\perp}$ is the orientational average of the projection of M_4 orthogonal to n, whereas $\mathcal{D}_{\mathrm{r},n}^{\parallel}$ is the projection of M_4 parallel to n. Intuitively, we expect the ratio $\mathcal{D}_{\mathrm{r},n}^{\perp}/\mathcal{D}_{\mathrm{r},n}^{\parallel}$ to be small when particles are compact in directions orthogonal to n, and relatively elongated in the direction of n. Mathematically, by properties of symmetric positive-definite matrices, the ratio $\mathcal{D}_{\mathrm{r},n}^{\perp}/\mathcal{D}_{\mathrm{r},n}^{\parallel}$ is minimized when n corresponds to an eigenvector of M_4 with the largest eigenvalue.

3.4. Properties of diffusion coefficients. Here we discuss various properties of the dimensionless scalar coefficients $\mathcal{D}_{\mathrm{t}}$ and $\mathcal{D}_{\mathrm{r},n}^{\perp}$ for a standard Stokesian hydrodynamic model. We discuss their dependence on the choice of particle reference point and particle frame, and in the case of $\mathcal{D}_{\mathrm{r},n}^{\perp}$ the dependence on the observation vector n.

Translational coefficient. Let $(\boldsymbol{r}', \boldsymbol{d}_i')$ and $(\boldsymbol{r}, \boldsymbol{d}_i)$ be two arbitrary points and frames fixed in a particle, and let $s = \ell^{-1}\xi \in \mathbb{R}^3$ and $\Xi \in \mathrm{SO}_3$ be the dimensionless components of the relative displacement and rotation as defined in section 2.2. Then from (2.17) we deduce that the dimensionless matrices M_1' and M_1 are related as

$$M_1' = \Xi^T\Big(M_1 + M_3[s\times] + [s\times]^T M_2 + [s\times]^T M_4[s\times]\Big)\Xi. \tag{3.40}$$

Taking the trace of (3.40) and using the facts that the trace is invariant under rotations and $M_2 = M_3^T$, together with the definitions of $[s\times]$ and $\operatorname{vec}[M_3 - M_3^T]$ and the epsilon-delta identity outlined in section 2.2, we deduce

$$\mathcal{D}_{\mathrm{t}}' = \mathcal{D}_{\mathrm{t}} - \frac{2}{3}\operatorname{vec}[M_3 - M_3^T] \cdot s + \frac{1}{3} s \cdot [\operatorname{tr}(M_4) I - M_4] s. \tag{3.41}$$

The main properties of the translational diffusion coefficient can now be stated. Specifically, from (3.41) we see that the coefficient is independent of the choice of particle frame, but is dependent on the choice of particle reference point. Indeed, because the matrix $[\operatorname{tr}(M_4)I - M_4]$ is symmetric and positive-definite, there is a

unique choice of reference point at which the coefficient achieves a minimum value. If the mobility matrix M is known at some given reference point $\boldsymbol{r}$, then by minimizing the expression in (3.41) over s, we find that the minimum value is achieved at the unique point $\boldsymbol{r}'$ defined by

$$s = [\mathrm{tr}(M_4)I - M_4]^{-1}\,\mathrm{vec}[M_3 - M_3^T]. \tag{3.42}$$

This point is referred to as the center of diffusion of the particle [6, 21]. By combining (3.42) and (3.41) we find that the minimal value is given by

$$\mathcal{D}'_{\mathrm{t}} = \mathcal{D}_{\mathrm{t}} - \frac{1}{3}\,\mathrm{vec}[M_3 - M_3^T]\cdot[\mathrm{tr}(M_4)I - M_4]^{-1}\,\mathrm{vec}[M_3 - M_3^T]. \tag{3.43}$$

From (3.42) and (3.43) we observe that the center of diffusion can also be described as the unique point at which the cross-coupling block M_3 and consequently M_2 is symmetric. For symmetric particles like spheres, ellipsoids, and straight cylinders, the center of diffusion is coincident with the center of volume. However, for particles of arbitrary shape, these two points are generally distinct.

Transverse rotational coefficient. As before, let $(\boldsymbol{r}', \boldsymbol{d}'_i)$ and $(\boldsymbol{r}, \boldsymbol{d}_i)$ be two arbitrary points and frames fixed in a particle, and let $s = \ell^{-1}\xi$ and Ξ be the dimensionless components of the relative displacement and rotation. Then from (2.17) we deduce that the dimensionless matrices M'_4 and M_4 are related as

$$M'_4 = \Xi^T M_4 \Xi. \tag{3.44}$$

Moreover, let $\boldsymbol{n}$ be a given unit vector with components n' and n in the frames $\{\boldsymbol{d}'_i\}$ and $\{\boldsymbol{d}_i\}$ so that $n' = \Xi^T n$. Then the associated projection matrices $P_{n'}$ and P_n satisfy

$$P_{n'} = \Xi^T P_n \Xi, \tag{3.45}$$

and combining (3.44) and (3.45), we find

$$P_{n'} M'_4 P_{n'} = \Xi^T P_n M_4 P_n \Xi. \tag{3.46}$$

The main properties of the transverse rotational diffusion coefficient can now be stated. Specifically, taking the trace of (3.46) and noting that the trace is invariant under rotations, we obtain

$$\mathcal{D}'^{\perp}_{r,n'} = \mathcal{D}^{\perp}_{\mathrm{r},n}. \tag{3.47}$$

Thus the coefficient is independent of both the particle frame and particle reference point and depends only on the unit vector $\boldsymbol{n}$. Moreover, from the definition of $\mathcal{D}^{\perp}_{\mathrm{r},n}$ in (3.39), we obtain the more explicit expression

$$\mathcal{D}^{\perp}_{\mathrm{r},n} = \frac{1}{2}[\mathrm{tr}(M_4) - n\cdot M_4 n]. \tag{3.48}$$

This shows that the coefficient achieves a minimum value when n corresponds to an eigenvector of M_4 with the largest eigenvalue. When M_4 has distinct eigenvalues, there is precisely one such independent eigenvector, and when M_4 has repeated eigenvalues, there is one or more such independent eigenvectors. In direct analogy to the center of diffusion which minimizes $\mathcal{D}_{\mathrm{t}}$, any unit vector n which minimizes $\mathcal{D}^{\perp}_{\mathrm{r},n}$ may be referred to as an axis of diffusion. For symmetric particles like ellipsoids and straight cylinders, the longest symmetry axis would be the axis of diffusion, and the longer this axis is compared to the others, the smaller the ratio $\mathcal{D}^{\perp}_{\mathrm{r},n}/\mathcal{D}^{\parallel}_{\mathrm{r},n}$ will be. For particles of elongated but arbitrary shape, we expect the direction of elongation to roughly correspond to the axis of diffusion.

4. Discussion. Here we use our results to examine various classic hydrodynamic methods for probing the structure of short, stiff DNA molecules up to about a persistence length.

4.1. Translational methods. Classic experimental methods based on translational motion include velocity sedimentation [14, 32, 35] and dynamic light scattering [3, 34]. The interpretation of experimental data obtained from these methods relies on the simplifying assumptions that translational and rotational motion at the relevant time scale can be treated as independent, and that the motion of a reference point in a particle is described by an isotropic diffusion equation with a scalar translational diffusion coefficient. Our results show that the simplifying assumptions are satisfied in a leading-order approximation with a diffusion coefficient $\mathcal{D}_{\mathrm{t}}$ as defined in (3.20), provided the parameter $\epsilon = \ell/L$ is small. Here ℓ is a characteristic length scale for a particle and L is a characteristic length scale for the spatial domain under observation in the experiment. We remark that if the point whose motion is measured is not known with certainty, then it is convenient to use the center of diffusion as the reference point. This yields the smallest possible value of $\mathcal{D}_{\mathrm{t}}$ for a given particle and guarantees that the theoretical diffusion coefficient is not overstated.

The validity of the simplifying assumptions for classic translational methods for DNA can now be examined. A characteristic length scale for a DNA molecule containing up to about 150 basepairs is the axial length, which is of the order $\ell = 10^{-8}$m based on a rise of 3.4Å per basepair [36]. A characteristic length scale for the spatial domain in velocity sedimentation is the size of the observed volume, which is of the order $L = 10^{-3}$m [14]. A characteristic length scale for the spatial domain in dynamic light scattering is the size of the illuminated volume, which is of the order $L = 10^{-4}$m [3, 34]. Thus for typical velocity sedimentation and dynamic light scattering experiments we estimate $\epsilon = 10^{-5}$ and $\epsilon = 10^{-4}$. Based on these estimates, for DNA molecules up to about a persistence length, we expect the simplifying assumptions to hold with high accuracy for both methods. Indeed, the analysis of experimental translational data in previous investigations of DNA [19, 39] and also proteins [2, 6, 16] supports the validity of the traditional diffusion model.

4.2. Rotational methods. Classic experimental methods based on rotational motion include electric dichroism and birefringence [13] and fluorescence polarization [40]. The interpretation of experimental data obtained from these methods relies on the simplifying assumptions that translational and rotational motion at the relevant time scale can be treated as independent, and that the motion of a distinguished axis or unit vector n (a dipole or polarization axis) is described by an isotropic diffusion equation on the unit sphere with a scalar transverse rotational diffusion coefficient. Our results show that the simplifying assumptions are satisfied in a leading-order approximation with a diffusion coefficient $\mathcal{D}^{\perp}_{\mathrm{r},n}$ defined in (3.39), provided the parameters $\epsilon = \ell/L$ and $\zeta_n = \mathcal{D}^{\perp}_{\mathrm{r},n}/\mathcal{D}^{\parallel}_{\mathrm{r},n}$ are small. Here ℓ and L have the same meaning as before and $\mathcal{D}^{\parallel}_{\mathrm{r},n}$ is the parallel rotational diffusion coefficient also defined in (3.39). If the axis whose motion is measured is not known with certainty, then it is convenient to use an axis of diffusion as the distinguished axis. This yields the smallest possible value of $\mathcal{D}^{\perp}_{\mathrm{r},n}$ for a given particle and guarantees that the theoretical diffusion coefficient is not overstated.

The validity of the simplifying assumptions for classic rotational methods for DNA can now be examined. As before, a characteristic length scale for a DNA molecule containing up to about 150 basepairs is $\ell = 10^{-8}$m. A characteristic length scale for the spatial domain in a typical rotational experiment is the size of the illuminated

volume, which is of the order $L = 10^{-3}$m [13]. Thus we have the estimate $\epsilon = 10^{-5}$, and the parameter ϵ is small regardless of the detailed shape of a molecule. In contrast, the hydrodynamic ratio ζ_n depends on the detailed shape and on the unit vector n. To explore the magnitude of this parameter, we employed a numerical procedure described in detail elsewhere [18, 19]. Specifically, we used a sequence-dependent curved tube model of DNA based on x-ray crystallography and an accurate boundary element technique to compute $\zeta_n = \mathcal{D}^{\perp}_{\mathrm{r},n}/\mathcal{D}^{\parallel}_{\mathrm{r},n}$ for random DNA sequences of different length: the coefficients $\mathcal{D}^{\perp}_{\mathrm{r},n}$ and $\mathcal{D}^{\parallel}_{\mathrm{r},n}$ were determined by the mobility matrix M_4 via (3.39), the matrix M_4 for a given sequence was determined by the Stokes flow equations as described in [19], and the Stokes equations were solved numerically using the boundary element technique described in [18]. For each sequence, we chose the unit vector n to be an axis of diffusion so that the value obtained for the ratio ζ_n was the smallest possible for that sequence.

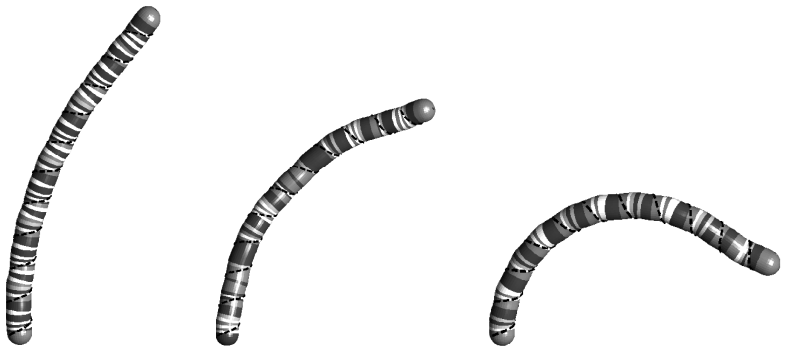

FIG. 4.1. *Curved tube models of three different* 120*-basepair sequences. The models shown have a tube radius of* 13*Å. The gray colors represent the sequence of bases along one strand (T = dark, A = medium dark, C = medium light, G = light), and the dashed curve on the surface illustrates the helical twist.*

Figure 4.1 illustrates the geometric model for some representative DNA sequences. The hydrated surface is modeled as a circular tube of uniform radius with ends capped by hemispheres. The axis of the tube is a space curve whose length and curvature are determined locally using a rigid basepair model of double-helical DNA in which the relative displacement and orientation between adjacent basepairs (dimer step) is described by a set of six parameters depending on the dimer composition [9, 11, 29]. The rigid surface is expected to provide a reasonable approximation for DNA fragments with length from about 20 to 150 basepairs. At longer lengths, we expect a flexible surface to be more appropriate, and at shorter lengths, we expect an atomistic-type surface which captures local fine-scale features to be more appropriate. For purposes of comparison, we also consider a classic straight tube model with length determined by the average separation distance or rise per basepair, which is about 3.4Å [36]. The tube radius in both the curved and straight models is a prescribed constant, with an estimated value in the range 10–13Å [19, 36, 39]. In our computations of ζ_n, we considered random DNA sequences of length $15, 20, 25, \ldots, 120$ basepairs, and for each length we generated a sample set of 50 sequences that were approximately uniformly distributed in radius of gyration.

Figure 4.2 shows computed values of the hydrodynamic ratio ζ_n versus length for both the curved and straight tube models. We plot the inverse ratio $1/\zeta_n$ rather than ζ_n since it enhances the sensitivity and makes the results more easily visible. The data

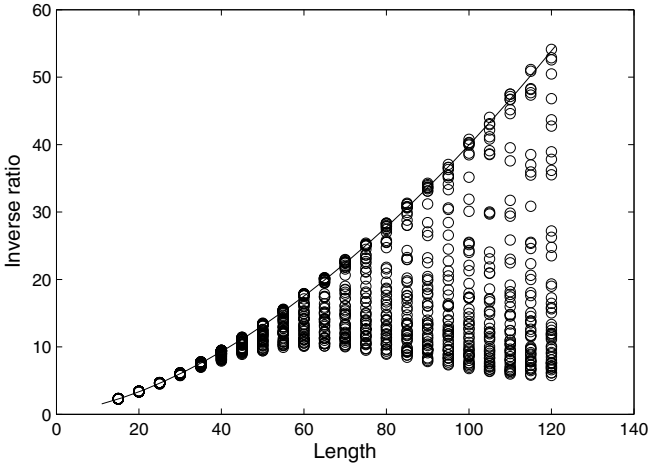

FIG. 4.2. *Inverse hydrodynamic ratio* $1/\zeta_n$ *versus length in basepairs. The open circles denote results for random DNA sequences of different length computed with the curved tube model with radius* $10\mathring{A}$*. The solid curve denotes results obtained from the straight tube model with the same radius.*

in the figure show that ζ_n is only moderately small for sequences corresponding to the upper envelope of the data, and is rather close to unity for sequences corresponding to the lower envelope. The solid curve near the upper envelope corresponds to results for the straight tube model. While the solid curve should presumably provide a strict upper bound on the data, small errors are visible due to small differences in the axial length of the curved and straight models. The local maximum visible in the lower envelope can be understood in terms of aspect ratio and axial curvature effects. Intuitively, the tubular geometry for sequences along this envelope is compact at short lengths, curved at long lengths, and elongated at intermediate lengths. The local maximum arises because $1/\zeta_n$ increases (ζ_n decreases) with elongation. The results shown correspond to a tube radius of 10Å. For larger values of the radius, we obtained similar results, but with lower values of $1/\zeta_n$ (higher values of ζ_n) for all but the shortest sequences.

The data in Figure 4.2 suggest that, for some sequences, the rotational motion measured by classic methods may not be accurately described by the traditional diffusion model. Indeed, the data show that the parameter ζ_n is highly variable and can be close to order unity depending on the sequence. We remark that 10Å is an effective lower bound for the radius of DNA based on x-ray diffraction data [36], and that a more realistic radius for DNA in solution is closer to 13Å [19, 39]. For this radius, the values of the parameter ζ_n would be larger, which would only strengthen our doubts. Indeed, discrepancies observed in the analysis of experimental rotational data in previous work [19] might be explained by the limited validity of the traditional model. We surmise that the accurate analysis of rotational data may require a diffusion model which accounts for self-coupling and other possible effects at the rotational time scale, which is of the order $t_{c,\mathrm{r}} = 10^{-5}\mathrm{s}$ for a DNA molecule of about one persistence length. A different hydrodynamic model and different interpretation of the hydrated surface may be required at this scale than at the much slower scales associated with translational data, which for velocity sedimentation is of the order $t_{c,\mathrm{s}} = 10^{2}\mathrm{s}$.

REFERENCES

[1] S. Allison, C. Chen, and D. Stigter, *The length dependence of translational diffusion, free solution electrophoretic mobility, and electrophoretic tether force of rigid rod-like model duplex DNA*, Biophys. J., 81 (2001), pp. 2558–2568.

[2] S. Aragon and D. Hahn, *Precise boundary element computation of protein transport properties: Diffusion tensors, specific volume and hydration*, Biophys. J., 91 (2006), pp. 1591–1603.

[3] B. Berne and R. Pecora, *Dynamic Light Scattering: With Applications to Chemistry, Biology and Physics*, Wiley, New York, 1976.

[4] H. Brenner, *Coupling between the translational and rotational Brownian motions of rigid particles of arbitrary shape*, I, J. Colloid Sci., 20 (1965), pp. 104–122.

[5] H. Brenner, *Coupling between the translational and rotational Brownian motions of rigid particles of arbitrary shape*, II, J. Colloid Interface Sci., 23 (1967), pp. 407–436.

[6] D. Brune and S. Kim, *Predicting protein diffusion coefficients*, Proc. Natl. Acad. Sci. USA, 90 (1993), pp. 3835–3839.

[7] C. Cantor and P. Schimmel, *Biophysical Chemistry, Part* II, W. H. Freeman, San Francisco, 1980.

[8] P. Debye, *Polar Molecules*, Chemical Catalog Company, New York, 1929.

[9] R. Dickerson, M. Bansal, C. Calladine, S. Diekmann, W. Hunter, O. Kennard, R. Lavery, H. Nelson, W. Olson, W. Saenger, Z. Shakked, H. Sklenar, D. Soumpasis, C.-S. Tung, and E. von Kitzing, *Definitions and nomenclature of nucleic acid structure parameters*, J. Mol. Biol., 205 (1989), pp. 787–791.

[10] A. Einstein, *Investigations on the Theory of the Brownian Movement*, Dover, New York, 1956.

[11] M. El Hassan and C. Calladine, *The assessment of the geometry of dinucleotide steps in double-helical DNA: A new local calculation scheme*, J. Mol. Biol., 251 (1995), pp. 648–664.

[12] L. Favro, *Theory of the rotational Brownian motion of a free rigid body*, Phys. Rev., 119 (1960), pp. 53–62.

[13] E. Fredericq and C. Houssier, *Electric Dichroism and Electric Birefringence*, Clarendon, Oxford, 1973.

[14] H. Fujita, *Foundations of Ultracentrifugal Analysis*, Wiley, New York, 1975.

[15] G. Galdi, *On the Motion of a Rigid Body in a Viscous Liquid: A Mathematical Analysis with Applications*, in Handbook of Mathematical Fluid Mechanics, Vol. 1, Elsevier, Amsterdam, 2002, pp. 653–792.

[16] J. Garcia de la Torre, M. Huertas, and B. Carrasco, *Calculation of hydrodynamic properties of globular proteins from their atomic-level structure*, Biophys. J., 78 (2000), pp. 719–730.

[17] H. Goldstein, *Classical Mechanics*, 2nd ed., Addison-Wesley, London, 1980.

[18] O. Gonzalez, *On stable, complete, and singularity-free boundary integral formulations of exterior Stokes flow*, SIAM J. Appl. Math., 69 (2009), pp. 933–958.

[19] O. Gonzalez and J. Li, *Modeling the sequence-dependent diffusion coefficients of short DNA sequences*, J. Chem. Phys., 129 (2008), article 165105.

[20] J. Happel and H. Brenner, *Low Reynolds Number Hydrodynamics: With Special Applications to Particulate Media*, Kluwer Academic, Boston, 1983.

[21] S. Harvey and J. Garcia de la Torre, *Coordinate systems for modeling the hydrodynamic resistance and diffusion coefficients of irregularly shaped rigid macromolecules*, Macromolecules, 13 (1980), pp. 960–964.

[22] H. Hinch, *Perturbation Methods*, Cambridge University Press, Cambridge, UK, 1991.

[23] P. Hughes, *Spacecraft Attitude Dynamics*, Wiley, Boston, 1983.

[24] S. Kim and S. Karrila, *Microhydrodynamics: Principles and Selected Applications*, Butterworth-Heinemann, Boston, 1991.

[25] S. Koenig, *Brownian motion of an ellipsoid: A correction to Perrin's results*, Biopolymers, 14 (1975), pp. 2421–2423.

[26] S. Mazur, C. Chen, and S. Allison, *Modeling the electrophoresis of short duplex DNA: Counterions K^+ and $Tris^+$*, J. Phys. Chem. B, 105 (2001), pp. 1100–1108.

[27] J. McConnell, *Rotational Brownian Motion and Dielectric Theory*, Academic Press, London, 1980.

[28] J. Munkres, *Analysis on Manifolds*, Addison-Wesley, New York, 1991.

[29] W. Olson, M. Bansal, S. Burley, R. Dickerson, M. Gerstein, S. Harvey, U. Heinemann, X. Lu, S. Neidle, Z. Shakked, H. Sklenar, M. Suzuki, C. Tung, E. Westhof, C. Wolberger, and H. Berman, *A standard reference frame for the description of nucleic acid base-pair geometry*, J. Mol. Biol., 313 (2001), pp. 229–237.

[30] J. Perrin, *Mouvement brownien d'un ellipsoide* (I). *Dispersion dielectrique pour des molecules ellipsoidales*, J. Phys. Radium, 5 (1934), pp. 497–511.
[31] J. Perrin, *Mouvement brownien d'un ellipsoide* (II). *Rotation libre et depolarisation des fluorescences: Translation et diffusion de molecules ellipsoidales*, J. Phys. Radium, 7 (1936), pp. 1–11.
[32] H. Schachman, *Ultracentrifugation in Biochemistry*, Academic Press, New York, 1959.
[33] J. Schellman and S. Harvey, *Static contributions to the persistence length of DNA and dynamic contributions to DNA curvature*, Biophys. Chem., 55 (1995), pp. 95–114.
[34] K. Schmitz, *Dynamic Light Scattering by Macromolecules*, Academic Press, San Diego, 1990.
[35] T. Schuster and T. Laue, eds., *Modern Analytical Ultracentrifugation*, Birkhäuser, Boston, 1994.
[36] R. Sinden, *DNA Structure and Function*, Academic Press, San Diego, 1994.
[37] C. Tanford, *Physical Chemistry of Macromolecules*, Wiley, New York, 1961.
[38] J. Thorpe, *Elementary Topics in Differential Geometry*, Springer-Verlag, New York, 1979.
[39] M. Tirado, C. Martinez, and J. Garcia de la Torre, *Comparison of theories for the translational and rotational diffusion coefficients of rod-like macromolecules: Application to short DNA fragments*, J. Chem. Phys., 81 (1984), pp. 2047–2052.
[40] B. Valeur, *Molecular Fluorescence: Principles and Applications*, Wiley-VCH, Weinheim, 2002.
[41] F. Verhulst, *Methods and Applications of Singular Perturbations: Boundary Layers and Multiple Timescale Dynamics*, Springer-Verlag, New York, 2005.